Muhammad Kashif Siddique

Aalto-1 CubeSat Mission Design Optimization

School of Electrical Engineering

Department of Electrical Engineering and Automation

Thesis submitted in partial fulfillment of the requirements for the degree of

Master of Science in Technology

Espoo, August 17, 2015

Supervisors: Professor Jaan Praks
Aalto University
School of Electrical Engineering

Professor Reza Emami
Luleå University of Technology

Preface

This thesis is submitted in partial fulfillment of the requirements for Joint European Master Degree in Space Science and Technology (Erasmus Mundus SpaceMaster program) at Aalto University, Finland and Luleå University of Technology, Sweden. It contains work done from February to August 2015.

I would like to thank my supervisor, Prof. Jaan Praks, for his support, valuable feedback and providing the opportunity to work with Aalto-1 CubeSat team. I would also like to thank Mr. Tomi Ylikorpi for his continuous help throughout the SpaceMaster program at Aalto University Finland. I would like to extend my gratitude to my SpaceMaster colleagues (Martin, Rokon, David, Rachit, Rian, Johnny, Thabet and Bagus) for the discussions and suggestions during the SpaceMaster program. I am grateful to my organization in Pakistan for providing immense support to complete my Joint European SpaceMaster studies.

Espoo, August 17, 2015

Muhammad Kashif Siddique

Aalto University
School of Electrical Engineering Abstract of the Master's Thesis

Author:	Muhammad Kashif Siddique
Title of the thesis:	Aalto-1 CubeSat Mission Design Optimization
Date:	August 17, 2015 **Number of pages:** 76
Department:	Electrical Engineering and Automation
Programme:	Master's Degree Programme in Space Science and Technology
Professorship:	Space Technology (S-92)
Supervisors:	Professor Jaan Praks (Aalto)
	Professor Reza Emami (LTU)

Small satellites are becoming increasingly popular solution for many space organizations and universities, both for commercial applications and scientific experimentation. The advances in electronics and sensor technology miniaturization have reduced the size of the satellites and enabled significant savings in construction and launch cost. However, the reliability and operability of very small satellites is still not in par with bigger satellites, tight budgets during the development and small amount of available energy in space set strong limits.

The aim of this thesis is to address the mission planning and scheduling problems of small satellites, especially the multi-objective missions that require advanced planning and scheduling methods to resolve the operational complexities with optimized utilization of available resources. The research compares two different satellite mission planning and scheduling techniques. First technique is the genetic algorithm (GA), a population based optimization of scheduling tasks, in which the fitness function is calculated by the weight factors assigned to each task depending upon the priority of the task. The second technique is heuristic approach using the constraint satisfaction problem (CSP) in which the sequences of actions are constructed based on other constraints, from initial state to desired goal. The optimized solution for the small satellite mission planning and scheduling of various mission phases has been implemented focusing on Aalto-1 CubeSat mission design. A mission simulation software toolbox, utilizing the mentioned optimization techniques, has been developed in order to provide mission analysis tools for CubeSats. Consequently, Aalto-1 CubeSat power budgets, on-board data budgets and communication schemes for UHF and S-band have been analysed to optimize the mission scheduling and planning for it's in-orbit operations. Furthermore, various design and operation phases have been explained in details to provide an overview of small satellites mission designs and to address the issues related to many CubeSat mission failures.

Keywords: Aalto-1, mission scheduling, small satellites, power budgeting, data budgeting, communication link budgeting, CubeSat

Contents

1 Introduction **1**

1.1 Introduction 1

2 Overview of Small Satellite Mission Design **4**

2.1 Small Satellite Mission Design 4

2.1.1 Mission Design Phase 4

2.1.2 Design of Operation Modes 6

2.1.3 Mission Planning and Scheduling 8

2.1.4 Satellite Mission Scheduling Optimization Techniques . . 10

2.2 Mission Scheduling using Genetic Algorithm 11

2.2.1 Fitness Function 11

2.2.2 Genetic Scheduling Algorithm 12

2.3 Mission Scheduling using Constraint-Based Approach 13

2.3.1 Constraint Satisfaction Problems 15

2.3.2 Constraint Modeling 15

2.3.3 Satellite Scheduling Constraints 17

3 Aalto-1 CubeSat Mission Overview **20**

3.1 Aalto-1 Mission Objectives 20

3.2 Aalto-1 CubeSat 21

3.2.1 Aalto-1 Payloads and Subsystems 22

3.2.2 General Design of EPS for Aalto-1 CubeSat 25

3.2.3 General Design of Aalto-1 OBC system 31

3.2.4 General Design of Aalto-1 Communication system 35

3.3 Ground Station 38

3.3.1 Aalto-1 Ground Station 39

4 Aalto-1 CubeSat Mission Managment **41**

4.1 Aalto-1 CubeSat Mission Management Strategy 41

4.1.1 Aalto-1 CubeSat Power Management 42

4.1.2 Aalto-1 CubeSat Data Management 45
4.1.3 Aalto-1 CubeSat Communication Management 46
4.1.4 Ground Visibility Time per Orbit 48
4.2 Aalto-1 CubeSat Orbit Simulations 50

5 Small Satellite Mission Simulations and Results 53
5.1 Simulations of Mission Schedule and Budgets 53
5.1.1 Simulation Results of Genetic Algorithm 53
5.1.2 Modeling of Constraint based Satellite Scheduling and Planning 59
5.2 Satellite Mission Planning Tool 60

6 Summary and Conclusions 67
6.1 Summary and Conclusions 67

References 71

List of Tables

2.1 Scheduling examples with their resources constraints 10

3.1 Aalto-1 spectral imager specifications [21] 22
3.2 Aalto-1 solar panel configuration details [31] 27
3.3 Aalto-1 battery specifications [29] 28
3.4 Technical specifications of Aalto-1 UHF radio transceiver [41] . . 37
3.5 Technical specifications of Aalto-1 S-Band radio transceiver [43] 38
3.6 Aalto-1 CubeSat ground station parameters 39

4.1 Estimated power required for AaSI operations 43
4.2 Estimated power required for RADMON operations 43
4.3 Estimated power required during communication phase 44
4.4 Estimated power required during electrostatic plasma brake experimentation 44

5.1 Mission scenario for GA simulations 54

List of Figures

1.1 Key factors for scheduling and planning of spacecraft mission . 2

2.1 Block diagram for mission design phase 5
2.2 Block diagram for launch and early orbit phase 6
2.3 Block diagram for service phase 7
2.4 Block diagram for satellite emergency modes 7
2.5 Block diagram for de-orbiting phase 8
2.6 Genetic scheduling algorithm block diagram 13
2.7 Block diagram of satellite task scheduling 14
2.8 Example of CSP planning model 16
2.9 CSP based schedule modeling approach 16

3.1 Aalto-1 CubeSat design overview [18] 21
3.2 Aalto-1 CubeSat ADCS design [27] 24
3.3 Aalto-1 EPS functional block diagram 25
3.4 Aalto-1 reference frame definition [18] 26
3.5 Aalto-1 solar panels [31] 27
3.6 CubeSat standalone battery by Clyde Space [33] 28
3.7 Aalto-1 CubeSat power requirements for different subsystems . 29
3.8 Aalto-1 CubeSat peak power vs standby power histogram . . . 30
3.9 Aalto-1 CubeSat power utilization summary for different subsystems 31
3.10 High-level block diagram of Aalto-1 CubeSat OBC [34] 32
3.11 Aalto-1 CubeSat OBC interfaces [36] 33
3.12 Aalto-1 CubeSat on-board telemetry data packet format 34
3.13 Aalto-1 on-board scheduler communication layer architecture . 35
3.14 Aalto-1 UHF radio communication system for telemetry/telecommand [42] 37
3.15 Aalto-1 CubeSat ground station architecture [47] 40

4.1 Aalto-1 CubeSat in-orbit mission phases 41

4.2 Eb/No vs bit error rate plot for uncoded coherent 4-PSK . . . 47
4.3 Comparison of digital modulation schemes for Eb/No and bandwidth efficiencies . . . 48
4.4 Orbital prediction tool (Gpredict) for the prediction of satellite passes using on-line NORAD TLE updates . . . 49
4.5 Aalto-1 CubeSat mission orbital simulation with Systems Tool Kit (STK) . . . 50
4.6 Aalto-1 CubeSat mission model for Euler angles . . . 51
4.7 Aalto-1 CubeSat change in angle between orbit plane and sun direction according to STK simulation . . . 51
4.8 Eclipse time plots of Aalto-1 CubeSat according to STK simulations . . . 52

5.1 Genetic Algorithm Matlab toolbox overview . . . 54
5.2 Genetic Algorithm simulation for fitness function best score optimization . . . 55
5.3 Genetic Algorithm simulation results for selection function . . . 56
5.4 Genetic Algorithm simulation results for the fitness function diversity score . . . 57
5.5 Genetic Algorithm simulation results for average distance b/w individuals . . . 58
5.6 Genetic Algorithm simulation results for selection of best individual . . . 59
5.7 CSP based modeling of satellite scheduling and planning . . . 60
5.8 Graphical user interface of satellite mission planning tool . . . 61
5.9 Orbital computation module of the satellite mission planning tool 62
5.10 Power budget module of the satellite mission planning tool . . . 65
5.11 Communication and data budget module of the satellite mission planning tool . . . 66

Symbols and Operators

P^0	genetic algorithm initial population
μ	size of population
λ	parental pool population size for genetic algorithm
Mem	memory size constraint
Pwr	power constraint
Pr	task priority constraint
TW	time window constraint
$Wthr$	weather condition constraint
$w1, ...w5$	weight factors
$Pwr_{produced}$	power produced per orbit
SP_{out}	solar panel output power
τ	orbital time period
β	angle between orbital plane and sun direction
t_{op}	operational time of satellite
t_{maxop}	maximum operational time of satellite
Pwr_{stored}	power stored in batteries
$P_1, P_2...P_n$	power modes for operations of satellite
N_B	number of batteries
N_c	number of battery cells
V_d	diode voltage drop
V_{dis}	battery cell discharge voltage
A_{sa}	solar array area
M_c	solar array mass
P_{EoL}	power produced at end of life
$b_1, b_2...b_n$	telemtry data packet bytes
C	checksum
R	radiud of Earth

Acronyms

AaSI	Aalto Spectral imager
ADCS	Attitude Determination and Control System
ADS	Antenna Deployment System
CDR	Critical Design Review
CSP	Constraint Satisfaction Problem
EM	Engineering Model
EPB	Electrostatic Plasma Brake
FM	Flight Model
GA	Genetic Algorithm
GPS	Global Position System
IOT	In-orbit Testing
LEOP	launch and early orbit phase
LEO	Low Earth Orbit
LVDS	Low-voltage Differential Signaling
NORAD	North American Aerospace Defense Command
NP	Non-deterministic Polynomial
OBC	On-Board Computer
PDR	Preliminary Design Review
QA	Quality Assurance

STK	Systems Tool Kit
TLE	Two Line Elements
UHF	Ultra High Frequency

Chapter 1

Introduction

1.1 Introduction

In recent years, there have been wide interest of many space research organizations in the development of small satellite solutions for their future missions. With the rapid development of technologies, the size of the electronic components used in the satellites is decreasing. These components have become also more power efficient in addition to their enhanced performance. This reduces the overall cost of missions and small satellite missions are becoming more common. Many universities are focused on the in-house hardware and software development of CubeSat (miniaturized satellite standard), resulting in significant advancement of CubeSat class satellites. Most of the small satellite missions are designed for the Earth observations but missions are also planned for the scientific explorations in the outer space [1].

As small satellite solutions are becoming more common, more and more organizations focus on the design and development of different subsystems of the satellite to enhance the capabilities of components like sensors, on-board electronics and mechanical structure. CubeSat development started in 1999, with the collaborative effort between California Polytechnic State University and Stanford University to standardize the cost effective design of pico-satellites. The main purpose of the standardization approach was to provide easier access to space for scientific research and to provide low cost piggyback launches [2].

Currently most small satellite developments addressing the issues related to the reliability, traceability, and re-usability. The mission design phases are more focused on avoiding the potential conflicts of different interfaces (different working modes, hardware and software failures). The system design phase also describes the estimation of the mission overhead in terms of power, telemetry, and computation associated with each component, interface, and task [3].

The satellite mission planning and scheduling is a complex problem of optimization and prioritization. The multi-objective missions require detailed planning and optimized scheduling of the tasks to perform efficiently and reduce the risk of anomalies. The key factors which play the main role in scheduling and planning of spacecraft missions are summarized in figure 1.1 [4].

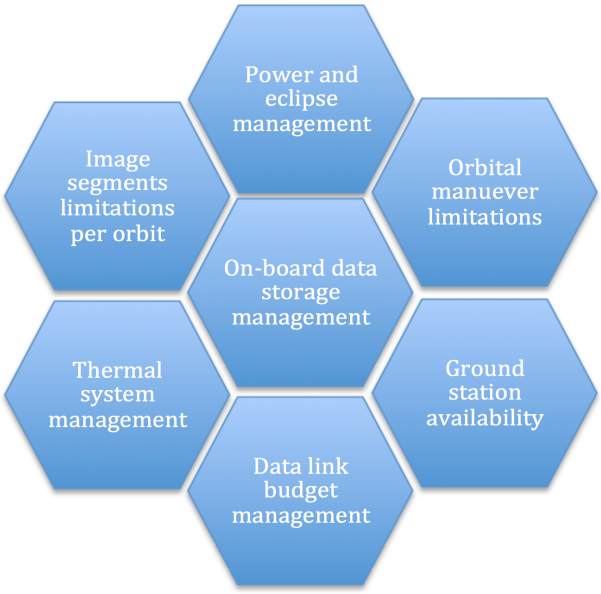

Figure 1.1: Key factors for scheduling and planning of spacecraft mission

The motivation behind this research is to develop an optimized solution for the small satellite mission planning and scheduling of various mission phases. The study is focused on the Aalto-1 CubeSat, which is under development in Aalto University, and is scheduled to be launched in late 2015. As Aalto-1 is multi-objective CubeSat with three different payload types (spectral imager, radiation

monitoring and plasma brake), for which an scheduling optimization method is required for the operation of successful mission. For this, different techniques of planning and scheduling optimization are studied and an optimal solution is developed for small satellites multi-objective missions, and as an example applied on the Aalto-1 CubeSat mission analysis, communication scheduling, mission phases scheduling, data budget scheduling and mission control software development.

For the methodology to address the planning and scheduling problem, two different algorithms are discussed. The first technique is based on the Genetic Algorithm (GA) which use the population-based method for the optimization of scheduling task [4] while the second technique is focused on a heuristic approach based on the Constraint Satisfaction Problem (CSP). These techniques are used to simulate power management, on-board data management and communication schemes, and compared.

Chapter 2

Overview of Small Satellite Mission Design

2.1 Small Satellite Mission Design

Most of the small satellites are launched in the Low Earth Orbit (LEO) for the Earth observations and different scientific experiments (e.g. solar radiation monitoring, deep space observations). In this chapter the different phases of small satellites development and in-orbit deployment are discussed at higher level based on the system engineering approach.

2.1.1 Mission Design Phase

In the design phase of a mission, the primary and secondary mission objective are described along with high level requirements of the mission. These high level requirements are used to achieve the objectives and facilitate the design. The high level requirements define the derived requirements which describe the mapping process for the implementation of subsystem designs and their interfaces with other components (e.g. peripheral components, sensors and communication interfaces). These mapping processes help to calculate different subsystems budgets like power requirements, memory requirements, data budgeting and communication link budgeting [5].

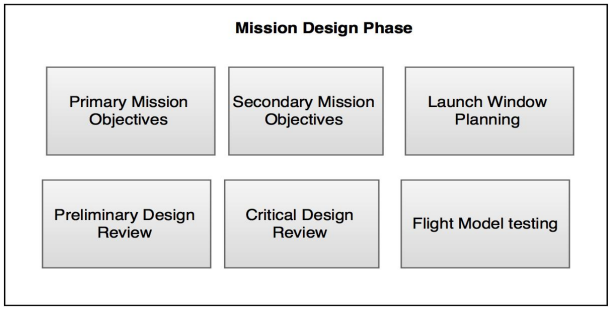

Figure 2.1: Block diagram for mission design phase

Both primary and secondary mission objectives and their derived requirements are discussed in detail during the Preliminary Design Review (PDR). The mapping process is scheduled for implementing the unit design, their interfaces with other components and integrated acquisition. All the risks, budgeting, schedule and technical details are also explained and discussed in detail during the PDR. While in the Critical Design Review (CDR), the maturity of the system units design are demonstrated. In CDR the Quality Assurance (QA) activities are also planned to ensure the quality of assembly, integration and testing of Engineering Model (EM) and Flight Model (FM). The ground station system development and operational activities are also assessed based on the allocated cost and schedules [6].

In many CubeSat projects traditional PDR/CDR phases are not followed which in some case caused the mission failures due to lack of micro-management of resources and document control. The EM and FM tests are also very important of mission design which should be documented and analyzed in detail [6]. These test results are very important during the in-orbit operation of satellite for the planning and scheduling of different task in case of anomaly. Therefore, PDR and CDR phases should be followed to increase the maturity of the system unit design, planned assembly, integration and testing [7].

After the assembly and integration, various tests are performed to ensure the quality of the FM. The most common tests include thermal vacuum chamber tests, out-gassing measurements, electromagnetic interference tests, antenna and RF tests.
The launch window is also planned along with selection of launch vehicle and

cost is negotiated with launching organizations. Usually the small satellites and CubeSats are launched as piggy back and many small satellites are launched using the single launch vehicle which help to reduce the launch costs [3] [8].

2.1.2 Design of Operation Modes

The in-orbit operation of satellite is divided into three major phases, launch and early orbit phase (LEOP), service phase and de-orbit phase.

Launch and Early Orbit Phase

The first operational phase is launch and early orbit phase (LEOP). The activities in this phase include the launch and in-orbit deployment of satellite and In-orbit Testing (IOT) of different subsystem. After the separation of satellite from launch vehicle, the communication module is switched on automatically. Satellite solar arrays and communication antennas are deployed. Initial orbital parameters are provided by launching organization to establish communication with satellite. After reaching the stable orbit, Attitude Determination and Control System (ADCS) confirms the Earth pointing for the communication of satellite. In the next stage, health check and testing of various scientific and payload equipment is performed before the service phase [9].

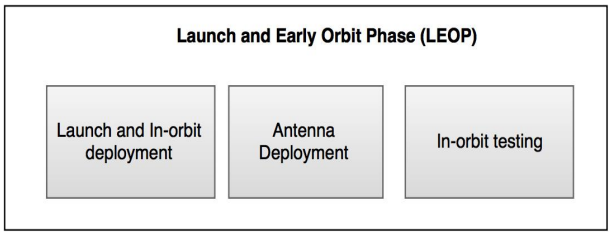

Figure 2.2: Block diagram for launch and early orbit phase

Service Phase

After the successful IOT, the payload is configured according to the mission objectives before the start its normal operations which starts the service phase. During the service phase, the satellite is maintained in the desired orbit using

the station keeping and satellite health is monitored by analyzing the telemetry data received on the ground station and power budgeting and on-board memory budgeting is performed based on the telemetry data for the completion of mission objectives. For the multi-objective missions, the different configurations are used according to operation schedule.

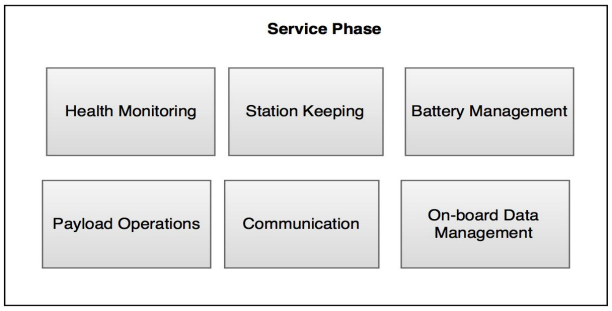

Figure 2.3: Block diagram for service phase

During the service phase the satellite health is constantly monitored whenever the satellite is visible from the ground station. In case of emergency, a heuristic approach is proposed in which the satellite changes its normal working mode to emergency mode. The emergency mode is usually divided into three different categories as shown in the figure 2.4. Each mode has different steps as shown in the figure 2.4 to perform on-board commands to address the anomaly and recover back to the normal mode [10].

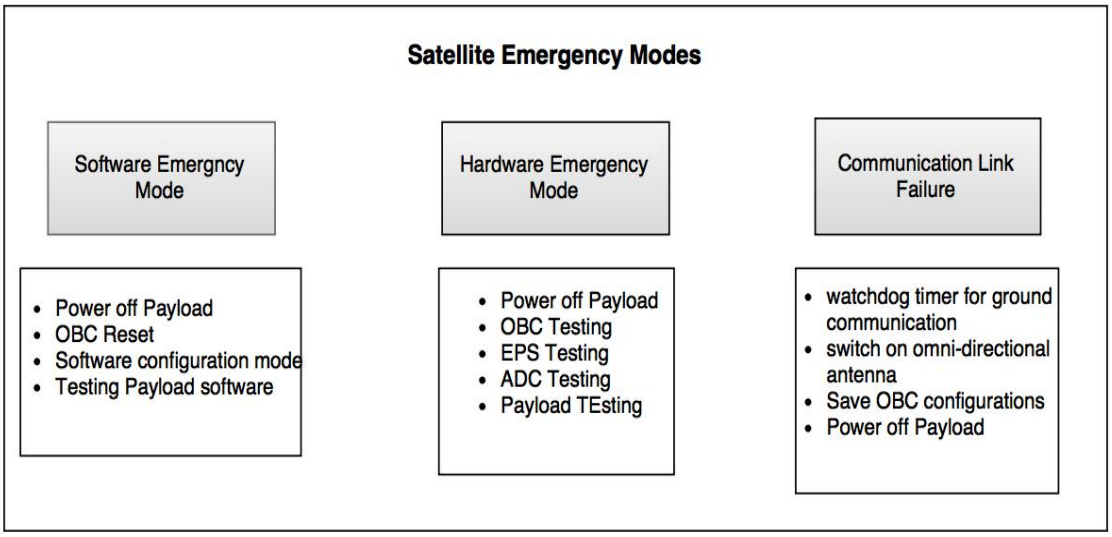

Figure 2.4: Block diagram for satellite emergency modes

De-Orbiting Phase

When the satellite mission is completed and it has achieved its mission objectives, the new orbit is planned and fuel budgeting is performed to de-orbit the satellite into the junk orbit and all the subsystems are switched off including the communication links, thus preventing the frequency interference with other satellites.

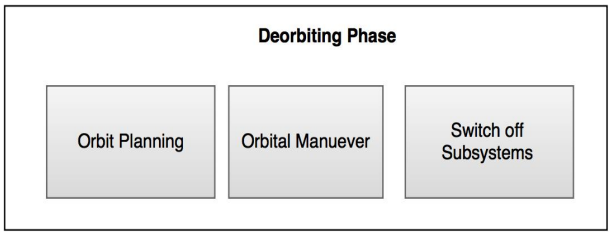

Figure 2.5: Block diagram for de-orbiting phase

2.1.3 Mission Planning and Scheduling

In order to switch optimally between operational modes and achieve the mission objectives, mission schedule has to be planned. For satellite mission planning and scheduling generally six parameters are taken into consideration which include orbital position, memory budgeting, power budgeting, task priority, time window and atmospheric conditions. These parameters play a key role for the scheduling of tasks considering the available resources and their constraints [11].

Orbital Position

Usually small satellites in the low Earth orbits have Global Position System (GPS) to determine their orbital position while some satellites using ranging data for the calculation of orbital parameters. The orbital parameters can also be used from North American Aerospace Defense Command (NORAD) where the Two Line Elements (TLE) are available for every satellite. Using current orbital parameters in the STK software, the orbital positions can be predicted along with the time window.The prediction data is used for the scheduling of genetic algorithm which compare the position of satellite with the area and orbital position constraints are removed using this process [11].

Memory Budgeting

Satellite on-board memory is also an important constraint for the successful mission objectives especially for the Earth observation satellites. The total memory available on-board is considered for the scheduling problems to record the SAR data and imaging. Due to memory limitations, the recorded data and imaging need to be transmitted to the ground station but the weight factor can be ignored in case of memory constraints for genetic algorithm scheduling [11].

Power Budgeting

Power management is also required for the satellite missions, as some instruments require more power than others and sometime the eclipse period add the complexity of the scheduling of this constraint [11].

Task Priority

Satellite missions also have some priority task for the observation of specific area or on-board bus data for the health monitoring and maintenance of satellite. Some payload tasks also need priority based on the customer request which add the complexity to the scheduling tasks. Satellite operations scheduling consider the task priority constraint as an important factor and genetic algorithm gives the one weightage to the priority task [11].

Time Window

The available time window is the key constraint for the scheduling problems and scheduler give the highest priority to the time based task to perform the desired task before the end time and scheduling of tasks are prioritized based on the end time in the time window [11].

Weather Conditions

Some Earth observation satellites depend on the weather conditions for their observation and for scheduling of such satellites, the weather constraint should also be considered. The task weighting factor can assigned depending upon the weather conditions. When there are dense clouds the task weightage can be reduced or mission task can be canceled from the scheduler [11].

2.1.4 Satellite Mission Scheduling Optimization Techniques

There are various algorithms and mathematical techniques for the optimized scheduling of satellite operational tasks. These algorithm manage the distribution of limited available resources over the tasks which are required to be executed for the successful achievement of mission's operations goals. The scheduling examples with their resources constraints are shown in the table 2.1

Name	Task	Resource Constraint
Ground Station	Telemetry and Tele-command	Event window, maintenance
Satellite	Remote sensing	Power, Memory
Launch Vehicle	In-orbit deployment	Fuel, Time window

Table 2.1: Scheduling examples with their resources constraints

For the spacecraft operations, time is the key factor and plays an important role for the planning and scheduling. The scheduling algorithm should generate the time line for the operations without overlapping the tasks and keeping in view of all the constraints because some tasks use the same resources for their execution. The scheduling tasks are also dependent on the satellite missions, for example in Earth observation satellites, the spectral imager operations is considered as main task for which the on-board memory and power are available resources while observation area, satellite orbit, memory size and priority are the constraints for the successful operation. The scheduling problems can be simplified by: [12]

- generating schedule for the satellite operations tasks in an ordered sequence,

- avoiding the overlapping of tasks,
- generating optimized time line with the available resources and constraints.

To address the problem of satellite mission scheduling and planning, two different approaches have been selected in this work based on their performance, customization and ability to handle the constraints without any overlapping and to optimize the resources utilization. The GA is an efficient approach to solve the scheduling problem for the optimization of complex multi-objective and multi-user tasks while CSP based scheduling provide the simple optimal solution to perform the satellite operations without any complexities [11][13].

2.2 Mission Scheduling using Genetic Algorithm

The concept of genetic algorithm (GA) is based on Darwin's theory of survival of the fittest [14]. The GA is used for both constrained and non-constrained based approaches for optimization. The algorithm continuously updates the changes in the population in a loop [15].

2.2.1 Fitness Function

Soon-mi Han et. al [11] proposed fitness function ($FitnessFunction$) for satellite scheduling based on the genetic based algorithm in which the constraints mentioned in the previous section are assigned weight factors. The generalized fitness function ($FitnessFunction$) is described in the equation

$$FitnessFunction = [(Mem \times w1) + (Pwr \times w2) + (((Pr - 10)^2) \times w3) + (((TW - 10)^2) \times w4) + (Wthr \times w5)] \times orb, \tag{2.1}$$

where, Mem is memory size, Pwr is available power, TW is the time window, $Wthr$ is weather condition factor and orb is the orbital position of satellite while

$w1, w2, w3, w4, w5$ are weighting factors assigned to each constraint.

The weight factor is assigned based on the schedule importance of the tasks and the highest value is given to tasks which have higher priority than the other tasks and those which have limited time window for the execution [11].

2.2.2 Genetic Scheduling Algorithm

The GA uses the fitness function which is constructed based on the different constraints of the problem and each constraint is given a specific weight factor based on its importance. The calculation of the fitness function is explained in detail later on. In GA, the initial population P^0 of size μ is evaluated and parental pool T^t of size λ is selected

$$T^t = Select(P^t). \tag{2.2}$$

After selecting parental pool T^t, the crossover procedure on the pairs of individual in T^t is performed taking the probability P_c^t as

$$P_c^t = Cross(T^t). \tag{2.3}$$

The mutation of individuals in P_c^t is performed with the probability of P_m^t which can be written in the form

$$P_m^t = Mutate(P_c^t). \tag{2.4}$$

The mutation P_m^t is evaluated and added as new population P^{t+1} with the size of μ and previous population number is replaced with the increment of t to $t+1$. This process is repeated until the best individual is found [4].

The GA take the random samples from the existing population as parents and produce children for next population and by repeating the same process, the population evolves toward an optimized solution [15]. The figure 2.6 show a block diagram for the satellite scheduling algorithm which is a heuristic approach by Soon-mi Han et. al [11]. In this scheduling algorithm the Non-deterministic Polynomial (NP) time are optimized. The optimization process

use the crossover, mutation and selection blocks as an operators for the efficient and reliable scheduling. The fitness function is computed by different weight factors assigned to each task and its constraints as shown in the figure 2.6.

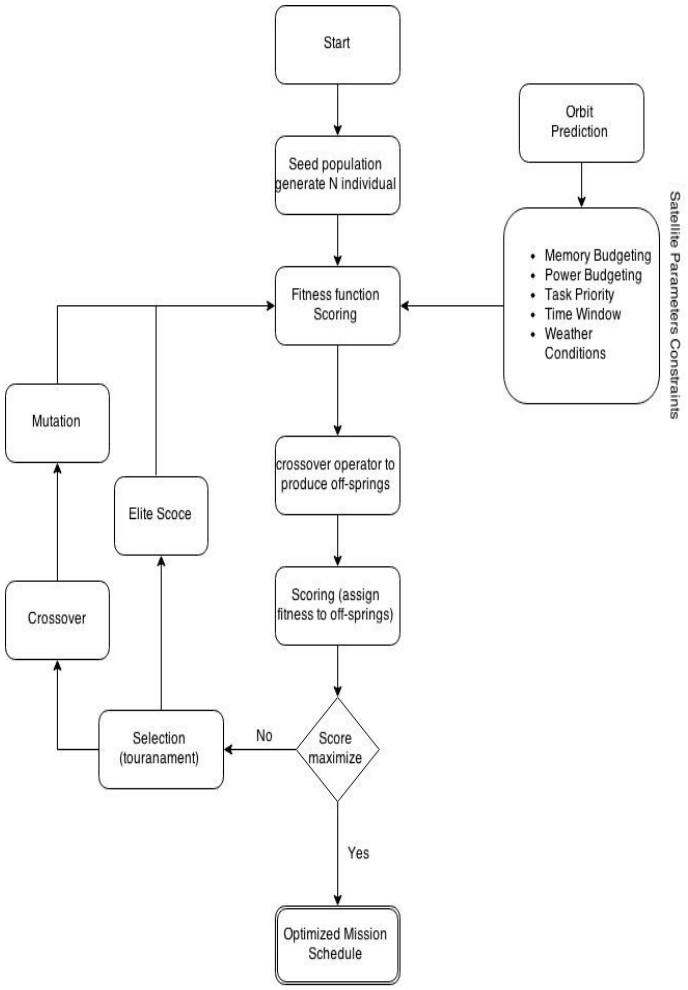

Figure 2.6: Genetic scheduling algorithm block diagram

2.3 Mission Scheduling using Constraint-Based Approach

Constraint based techniques are very useful for the planning and scheduling of tasks. In planning of task, a sequential actions are constructed for the initial state to the desired goals which are needed to be achieved while in scheduling task, the desired actions are allocated with respect to the available resources and time. In constraint based algorithms, task modeling and solving the prob-

lems with the optimized combinatorial is usually very efficient. The constraint based approach serve as bridge between planning and scheduling of task [16].

Most of the in-orbit operations contain the following tasks as shown in the figure 2.7. These operations include the scheduling of LEOP and normal in-orbit operations. The constraint based approach can be used of small satellite missions for Earth observations as well as for geostationary satellites.

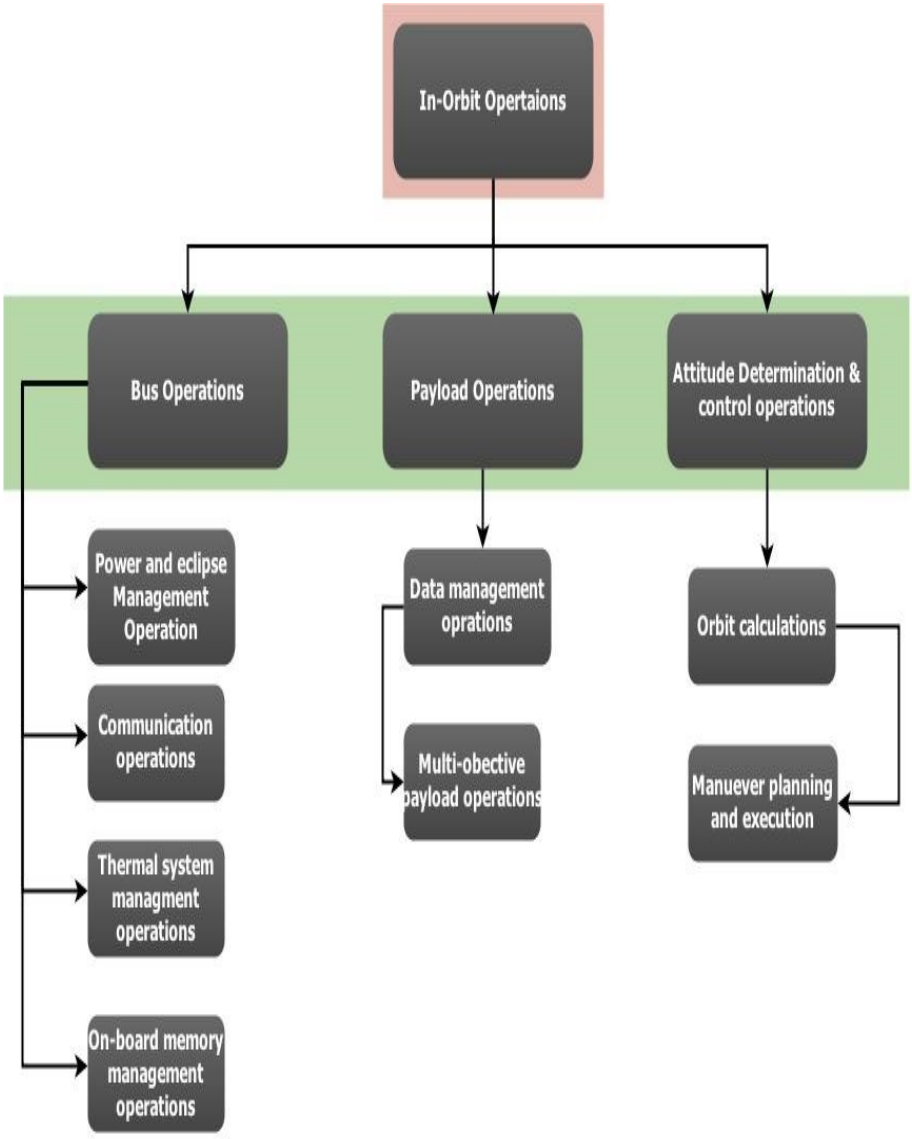

Figure 2.7: Block diagram of satellite task scheduling

Most of the Earth observation satellites are in the LEO and do not have ground station visibility all the time. So during limited visibility window, the scheduling

tasks needed to be optimized for the efficient operations. Due to time and bandwidth limitations, priority system can be used for the planning and scheduling of tasks. For the optimized operations each task can be assigned with priority weightage to perform the operation in the visibility window [13].

2.3.1 Constraint Satisfaction Problems

Constraint satisfaction problem (CSP) can be defined as the set of n number of variables which are associated to a domain and a set of constraining relations each involving subset of the variables, in which each possible n-pair is an instantiation of the n variables which satisfy the relations [17].

2.3.2 Constraint Modeling

Classical planning can be modeled using constraint based algorithm by creating shortest sequence of actions which transform the initial state of task to the desired goal state while the state can be described by the set of multi-valued variables and the actions can be described by the preconditions which are the desired values of state variables before the execution of action and the effects which describe the state variable values after the execution of action [16].

For example an Earth observation satellite need to take images of at target location while orbiting around the Earth and store the image in the memory. This problem can be modeled as shown in the example in figure 2.8.

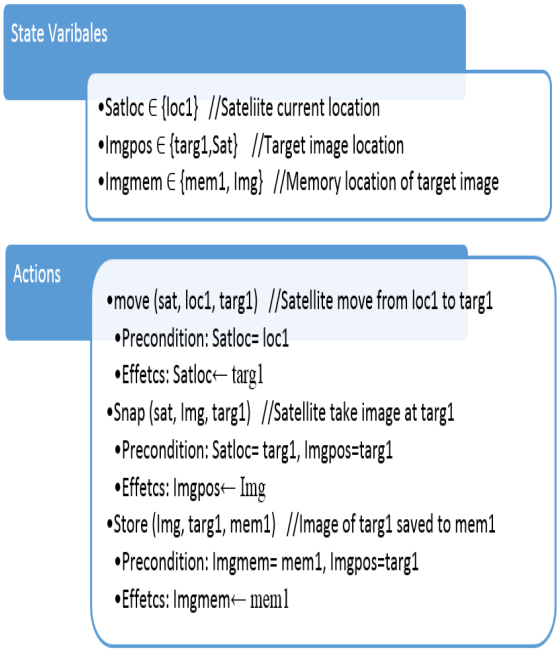

Figure 2.8: Example of CSP planning model

One simple approach for the satellite scheduling is to develop the CSP model of the tasks and then solving the CSP models. The satellite scheduling tasks can be modeled by using four objects as shown in the figure 2.9. For the scheduling of task, resources are assigned to it with event occurrence considering all the constraints.

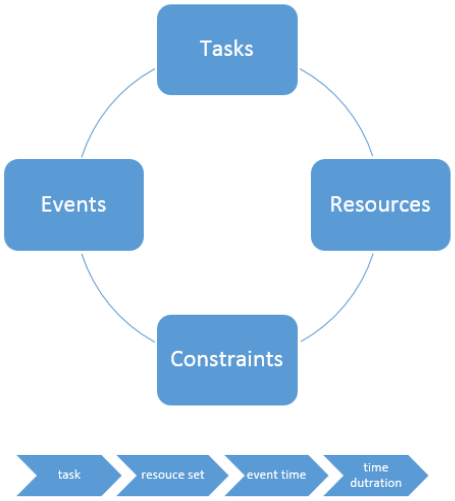

Figure 2.9: CSP based schedule modeling approach

For CSP model of satellite scheduling, resources can be considered as available bandwidth , sensors, antennas and ground station availability. Sometimes resources also need to perform some tasks which can be described as priori, in this case the scheduling problem is simplified by finding the task activity time and its duration [13].

2.3.3 Satellite Scheduling Constraints

The satellite scheduling constraints can be categorized into three main types, which are task constraints, event constraint and resource constraint. In task constraint two different tasks needed to be performed at the same time while in the resource constraint, same resource required to be used by two different task at the same time. When satellite visibility window is available from the ground station and multiple task needed to performed in the limited time duration which are event constraint problems. Based on these satellite scheduling categories the scheduling problem can be characterized by following properties [13].

Periodic Tasks

After in-orbit deployment of satellite, the routine maintenance operations have some periodic tasks which increase the complexity of satellite scheduling problems. Some common periodic tasks include the memory download, orbital maneuvers and multi-objective payload management. Some of periodic tasks are time based while others are event based. Time based periodic task can be managed by the on-board scheduler and these tasks can also be executed when there is no visibility with the ground station. The event based periodic tasks first need to determine their event constraint after which these task can be executed. Some periodic task require the information of previous executed task for their successful execution [13].

Preemptive task

During the satellite operations some tasks are given the priority over the regular tasks. For example preemptive task for Aalto-1 CubeSat can be given as Aalto-1 spectral imager must observe the Baltic area during next 48 hours of Earth observation.
The preemptive tasks can be divided into subtasks with shorter durations for each subtask to optimize the scheduling so that the resources can be used for the other scheduled tasks. The preemptive tasks can be scheduled based on the order of subtasks and when the subtasks are too large to find schedule in the specific time then iterative approach can be used in which initial subtasks numbers are small and increased gradually to optimize the schedule [13].

Variable length tasks

Some of the tasks require variable time duration for their execution. For this kind of tasks the satellite scheduler should decide the duration for a task along with the required resources to optimize the scheduling problem. Satellite scheduler need an extra decision making level for the duration assignment of the task. Although variable length tasks add complexity to the scheduling problem and cannot be optimized and heuristic approaches can be used for the scheduling this kind of tasks [13].

Renewable Resources

As satellite scheduling require resources for the execution of the tasks and some of satellite resources are renewable for example battery power and on-board memory. The renewable resources also need detailed scheduling for the optimization of other tasks because they play a critical role for the task execution. Consider a satellite is in eclipse for some time duration and two observation tasks are scheduled during this time with limited battery power. The satellite scheduler should manage tasks and its time duration in an optimized way considering the power constraints. Similarly the satellite memory need to be optimized considering the limited communication channels constraints and on board memory size constraints.

The preemptive and periodic tasks scheduling also add the complexity to the renewable resources management. There two different heuristic approaches are discussed by Joseph C. Pemberton et. al.[13].
In the first approach the minimum number of tasks for each renewable resource are used for the scheduling. If the schedule is not feasible, then the number of tasks are incremented for each renewable resources and scheduling performed. This method is repeated until the optimized solution is found. While in the second approach, some tasks for each renewable resource are generated and then optimize the feasible solution which uses as few tasks as possible [13].

Event Window

The event window is the time duration when the satellite is visible to the ground station which is dependent on the orbital period. The event window is an important constraint of satellite scheduling task. The prediction orbital parameters are used for the calculation of task scheduling and available time duration of the event window. A set of times can be selected to perform the tasks, for optimized execution of task, an auxiliary task variable should be used for the scheduler which select the event window time for task execution [13].

Chapter 3

Aalto-1 CubeSat Mission Overview

Aalto-1 is a student built nanosatellite which is being developed at Aalto University and expected to be launched by the December 2015. Here the Aalto-1 CubeSat mission is taken as a case study for the application of small satellite mission scheduling and planning solutions. In this thesis the power budgets, data budgets and communication schemes for Aalto-1 CubeSat are discussed with respect to mission planning and scheduling [18].

3.1 Aalto-1 Mission Objectives

Aalto-1 CubeSat is an educational satellite which has multi-objective missions with the goals to achieve the technology demonstration of science missions for Electrostatic Plasma Brake (EPB) experimentation and RADMON experimentation to study the radiation belt of electrons and protons for the duration of the mission. Another objective of the mission is to demonstrate the operation of a novel staring imaging spectrometer in the nanosatellite. Aalto-1 CubeSat is designed for the operational life of 2 years and in first six to twelve months the primary goals related to remote sensing using Aalto Spectral imager (AaSI) (developed by VTT) and radiation monitoring using RADMON (developed by University of Helsinki) will be accomplished and later on plasma brake technology demonstration experiments using EPB (developed by Finnish Meteorological Institute) will be performed. The satellite is planned to be launched in

sun-synchronous orbit with altitude from $500 - 900\ km$. The satellite has an accurate attitude determination and control unit while GPS unit is integrated in the satellite for the positioning of satellite and NORAD TLE will be used as backup for the positioning system. The communication system have Ultra High Frequency (UHF) and S-band modules for the housekeeping and payloads data respectively [18][19].

3.2 Aalto-1 CubeSat

Aalto-1 CubeSat is designed according to 3U CubeSat nanosatellite specifications having 4 kg of mass. The dimensions of the Aalto-1 structure is $10 \times 10 \times 34\ cm^3$. The outer structure is made of 1.5 mm thick aluminum parts which are tied together to form tube like shape while the inner structure have stacks which are designed to fit in with the printed circuit boards (PCB) and other components conforming the CubeSat technical requirements as shown in the figure 3.1. Aalto-1 CubeSat will be launched in the sun synchronous LEO. After assembly and integration of components, the satellite will be sealed in the protection pod which protect the satellite within from the other nanosatellites and launcher as well. The pod conforms all the standards of CubeSat specifications for the deployment [18].

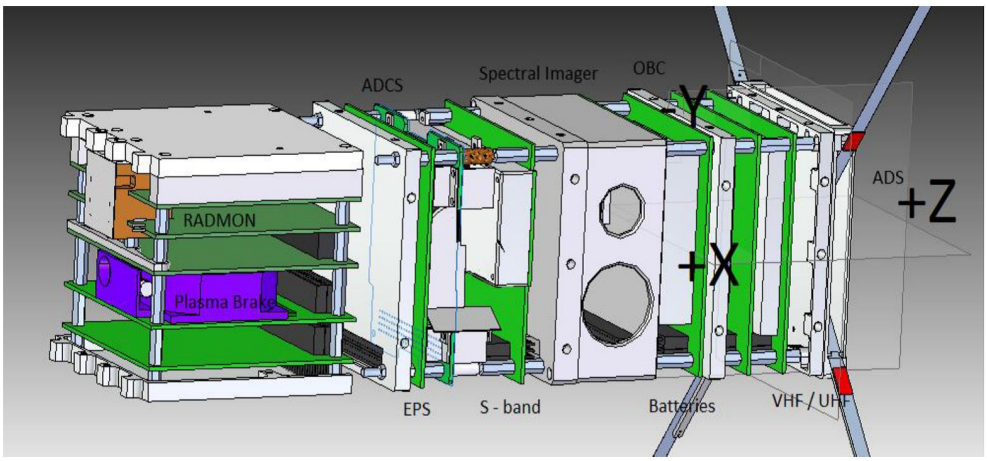

Figure 3.1: Aalto-1 CubeSat design overview [18]

When the Aalto-1 will be deployed the desired orbit it will maintain the same orbit during the first planned science mission to accomplish the primary ob-

jectives by providing the remote sensing data and radiation monitoring data. However, in the last part of technology demonstration, the plasma brake experiment will be performed which will change its orbit altitude resulting the change in the other orbital parameters due to the drag force caused by the tether. As the final orbit is uncertain and orbital parameters are not known which can affect the efficiency of various subsystems like power generation and thermal system for which Aalto-1 CubeSat is designed with a 20% margin, so that the mission can continue in a sun-synchronous orbit with a significantly differing β angle. The outer structure of satellite will be covered with the different sized solar panels, three long-side solar panels, and one smaller on the nadir side. The solar panels will produce an average power of 4.5 W at an altitude of 500 km at the end of life and during eclipse period the satellite will use the power from batteries [18] [20].

3.2.1 Aalto-1 Payloads and Subsystems

The brief description of different subsystems of Aalto-1 CubeSat as shown in figure 3.1 is given below;

Aalto-1 Spectral Imager

Aalto-1 spectral imager (AaSI) is a Piezo-actuated, tunable Fabry-Perot interferometer (PFPI). It consists of two reflectors that are separated by an air gap and it can capture two-dimensional spatial images up to three wavelengths at the same time. The CMOS color image sensor is used for the matching of multiple orders of FPI transmission based on the CMOS sensitivities. The data is collected using the multi channels at the same time. The same image sensor is also used for the visual camera. Some properties of AaSI are tabulated as shown in the table 4.1[21] [22].

Specification	**Units**
Sensor Image pixel	2048×2048
Delivered spectral image	512×512

Table 3.1: Aalto-1 spectral imager specifications [21]

RADMON

The radiation environment in LEO has proton (10–200 MeV) and electron (0.7–10 MeV). The radiation monitor instrument RADMON consists of a miniature instrument, which has thin silicon detector that can measure the proton and electron energy loss while thick cesium scintillator is combined with a photodiode to measure the remaining energy of the particles trapped in the telescope. The telescope consists of two units, one is analogue board for the detection, amplification and digitization of the signal while the other one is FPGA board for the processing of the signal. The primary goal of RADMON is the technology demonstration for the scientific missions[18][23].

Plasma Brake

EPB is the technology demonstration of the electrostatic plasma brake based on the e-sail concept for the efficient interplanetary travel [24]. During plasma brake experimentation, GPS will be used once per orbit to roughly estimate the change in the orbital position. The plasma brake instrument has long tether which can be positively or negatively charged which reacts with the ionosphere in the orbit causing the Coulomb drag force [25][26].

ADCS

Aalto-1 CubeSat has an active attitude determination and control system (ADCS), which is designed and manufactured by Berlin Space Technologies. For ADCS, Berlin Space Technologies has developed a board iADCS-100 whose architecture is shown in the figure 3.2. The iADCS-100 has magnetometers, MEMS gyros, sun sensors and reaction wheels to control the satellite with less than one degree pointing accuracy. During the first phase of satellite mission, pointing accuracy required to be less than 10° while the EPB experiment require rough estimation of attitude information. A star tracker is also part of iADCS-100 which improves the attitude data results [27].

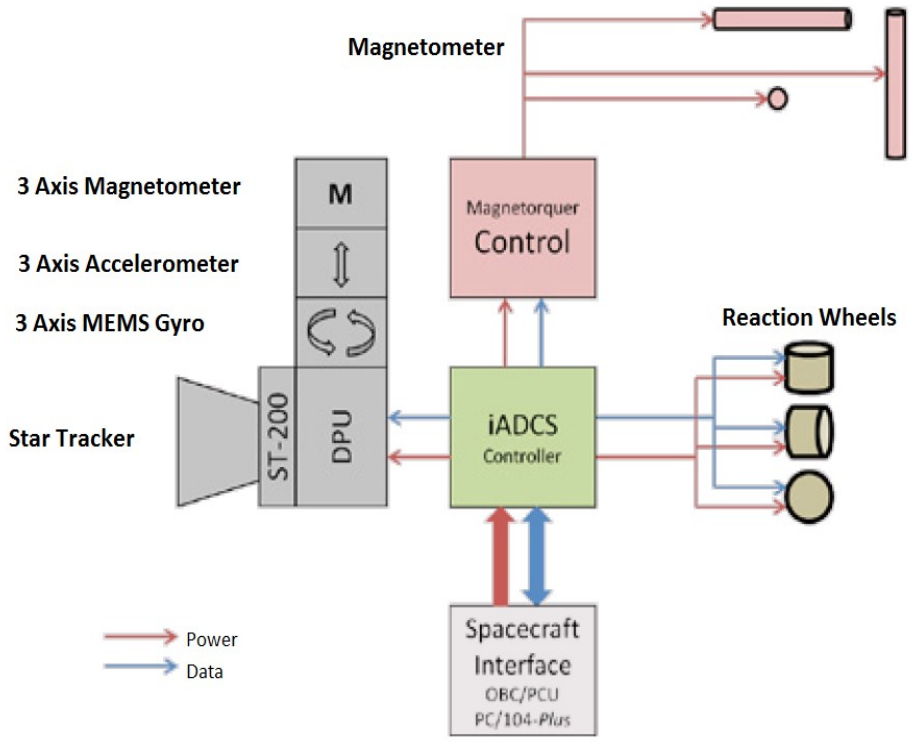

Figure 3.2: Aalto-1 CubeSat ADCS design [27]

During the operation when high accuracy data is required, the star tracker will be used as primary unit along with the reaction wheels to acquire more precise data and pointing accuracy. The magnetometers provide the lass pointing accuracy as compared to reaction wheels, which will be used in the later phase of operation when the plasma brake experimentation will be performed [18].

GPS

Aalto-1 CubeSat is also equipped with GPS receiver which provide the positional information to track the satellite and for the calculation of orbital parameters. The GPS receiver used in the Aalto-1 CubeSat is developed by Fastrax and will be used as primary source for the positional information while NORAD TLE will be used as backup for the prediction of orbital parameters so that ground station can establish the communication link as per visibility schedule [18] [28].

3.2.2 General Design of EPS for Aalto-1 CubeSat

Aalto-1 Electrical Power System (EPS) is an important subsystem which provide the power control of all the subsystem through OBC. The EPS not only distribute the power to all subsystems but also generate and store the power through solar panels and battery. Therefore optimized power management of EPS play a key role for the success of mission.

Aalto-1 EPS is designed for the fully functional subsystems at the end of the mission (EOL), which are estimated 2 years after launch. The general block diagram of Aalto-1 EPS is shown in the figure 3.3. in which solar panel are connected to battery charge regulators (BCR) through electrical power system control board (EPSCB). The BCR convert the input power from the solar panel to the required charging voltage for the lithium polymer battery cells. The EPS control board has power conditioning module (PCM) which used the step down converters for the distribution of $+3.3\ V$ and $+5\ V$ to the EPS bus while battery board has step-up converter which provide the $+12\ V$ supply to the EPS bus system. The satellite EPS bus has dedicated power lines to other subsystems as per voltage requirement of the units to distribute the power supply to the all the subsystems[29].

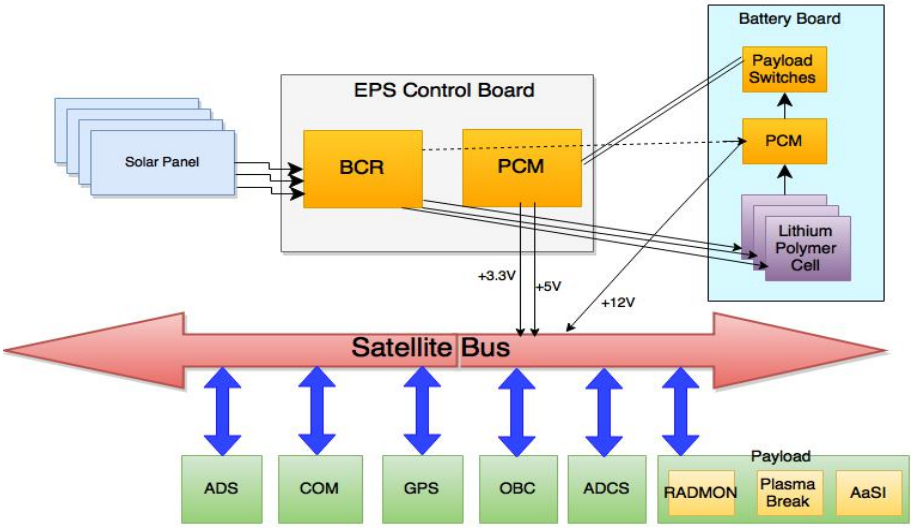

Figure 3.3: Aalto-1 EPS functional block diagram

The Aalto-1 EPS will produce the orbit average power (OAP) of 5 W during

the single orbit and the average power will also remain almost same in EOL. I^2C is used for the interfacing of OBC and EPS while EPS is configured as slave. The data communication rate between OBC and EPS is 100 $Kbps$ and EPS provide the telemetry data regarding the solar panel voltages, currents and temperatures, individual battery cell voltage and current levels, battery bus current, temperature of each battery and battery charge/discharge status for each battery upon the request from OBC. The OBC can also send command to control the power switches of different units like RADMON, AaSI, communication and ADCS subsystems. A watchdog timer is also configured in case of failure of OBC to EPS communication which will hard reset the OBC or any other subsystem malfunctioning[29].

Solar Panel Output

The Aalto-1 EPS solar cells are manufactured using GaInP/GaAs/Ge material and have a minimum efficiency of 25% in End of Life (EOL) while the solar cells have Beginning Of Life (BOL) efficiency of 29.5% and BOL power of 1.2 $W/cell$. Although the solar panel can produce upto 20 W of power theoretically when satellite is in sun synchronous orbit and all the cells are facing sun but due to degradation and other factors, they will produce at least 5 W of power in EOL. The figure 3.4 shows the orientation axis of the satellite which is helpful to understand the solar panel configuration. The sun sensors and temperature sensor are also integrated integrated into the solar panels for design optimization [29][30].

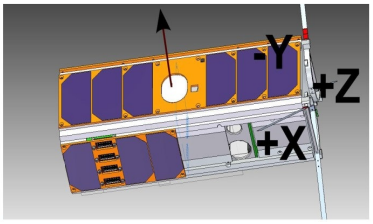

Figure 3.4: Aalto-1 reference frame definition [18]

The following table 3.2 shows the solar panels configurations, power output along with glass cover types and mass of solar cells used in the solar panels of Aalto-1 EPS.

Panel	Solar Cell	Power Output	Mass
+X-panel	2 cells with conductive cover glass	2.5 W	50 g
-X-panel	8 cells with normal CMG cover glass	9.9 W	170 g
+Y-panel	8 cells with normal CMG cover glass	9.9 W	170 g
-Y-panel	6 cells with conductive cover glass	7.4 W	150 g

Table 3.2: Aalto-1 solar panel configuration details [31]

The following figure 3.5 shows the Aalto-1 solar panels during the flight model testing.

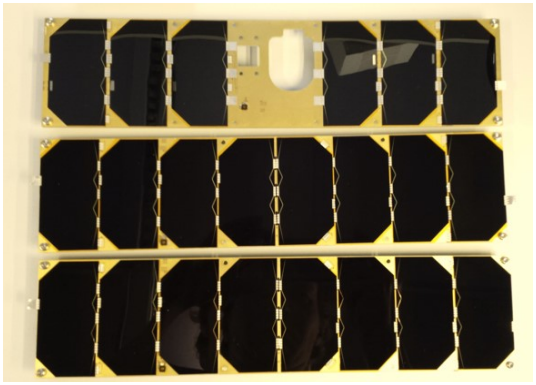

Figure 3.5: Aalto-1 solar panels [31]

Battery

Aalto-1 EPS has lithium polymer battery cells with the total capacity of 30 Wh. The battery board is manufactured by Clyde Space. The figure 3.6 show the battery made Clyde Space which is providing +12 V power line to the satellite bus and Battery Charge Regulator (BCR) are connected with lithium polymer cell for storing the charge with a charging connector of +5 V [32].

Figure 3.6: CubeSat standalone battery by Clyde Space [33]

The following table 3.3 shows the operational specifications for Aalto-1 EPS. It is recommended by the manufacturer that the maximum DoD should not exceed 20% [29].

Capacity	**Nom. Voltage**	**DoD**	**charge/discharge rate**	**Temp.**
30 Wh	8.4 V	20 %	3.75 A	$-10°to50°$

Table 3.3: Aalto-1 battery specifications [29]

Power Requirements for Subsystems

Aalto-1 EPS manage the power requirements of all the subsystems for the successful operations of the CubeSat. The power requirements of various subsystems and payload modules are described in the figure 3.7. The power requirements have been divided into two operational modes; standby power and peak power. The total peak power required by the CubeSat is 23.03 W while the standby power required is 3.295 W [18].

POWER REQUIRED BY EACH SUBSYSTEM

Subsystem	Standby Power (W)	Peak Power (W)	Remarks
ADS	0	7	for 60 seconds
ADCS	0,5	1,8	Sun Sensor require 0,06 W
GPS	0,045	0,13	active antenna and receiver
OBC	0,250	0,55	
UHF System	0,2	1,55	
S-Band System	0	3,5	
RADMON	0	1,5	Target Tracking require extra 0,45 W
AaSI	0	4	
Plasma Brake	2,3	3	
Total	3,295	23,03	

Figure 3.7: Aalto-1 CubeSat power requirements for different subsystems

The histogram in the figure 3.8 illustrates the comparison of Aalto-1 CubeSat peak power vs. standby power of each subsystem. The Antenna Deployment System (ADS) require 7 W peak power and it does not require any standby power because after the deployment of antennas, this subsystem is turned off. The GPS, OBC and UHF communication systems require less than 0.3 W of standby power for each subsystem respectively. AaSI, RADMON and S-band communication systems does not require any standby power for their in-orbit operations. EPB require maximum standby power of 2.3 W as compared to other subsystems while the peak power required for EPB is 3 W.

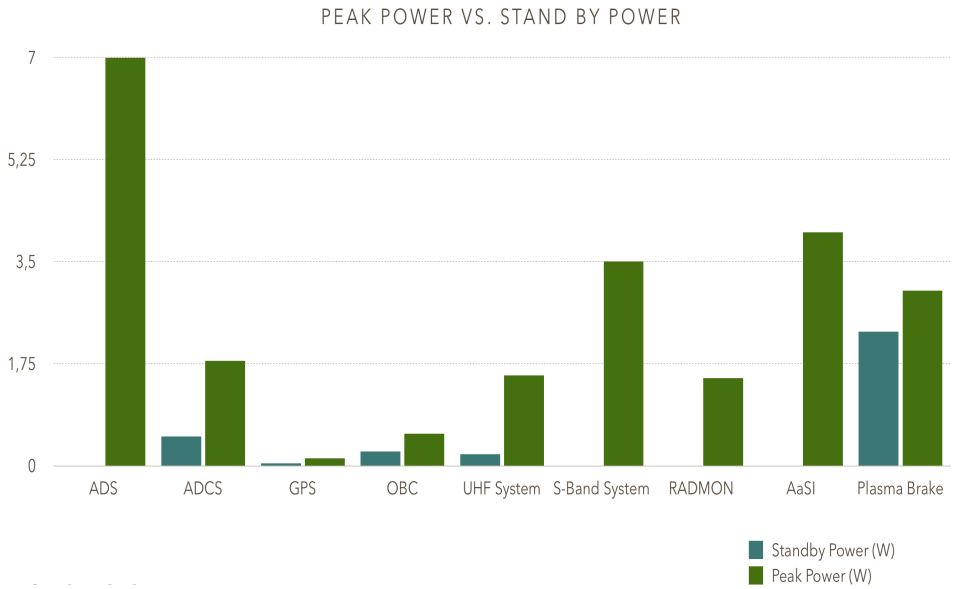

Figure 3.8: Aalto-1 CubeSat peak power vs standby power histogram

The figure 3.9 shows the power utilization of each subsystem. ADS utilize maximum power of 30% but the operational time for the ADS is about 60 seconds during LEOP. AaSI utilize the 17% of the power for its in-orbit operations. The S-band communication system utilize 15% of the power as compared to the 7% utilization of UHF communication system because S-band communication require more power to transmit the high data rate with the higher frequency signal. EPB and RADMON utilize 13% and 7% power respectively. The On-Board Computer (OBC) and GPS are using minimum powers of 2% and 1% respectively as compared to other subsystems.

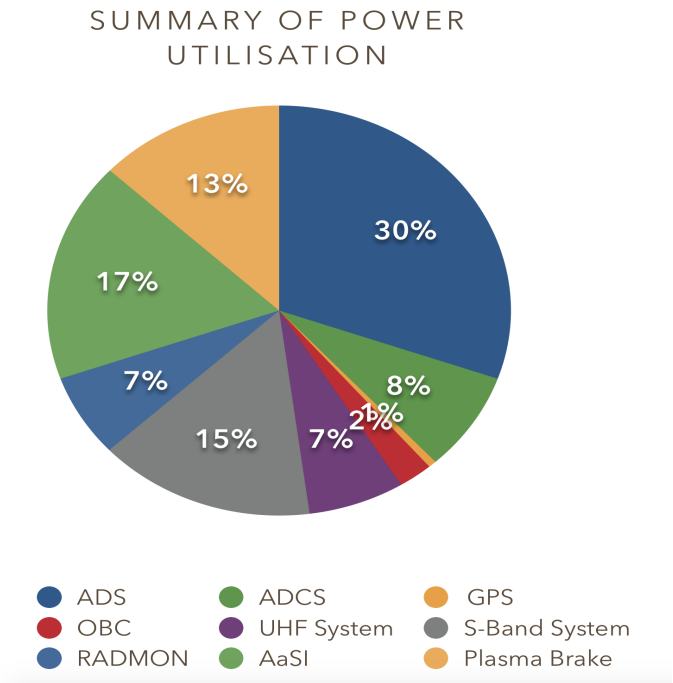

Figure 3.9: Aalto-1 CubeSat power utilization summary for different subsystems

3.2.3 General Design of Aalto-1 OBC system

OBC is main subsystem of satellite as it has interfacing with all the subsystems for communications to manage the various components. The high-level block diagram of Aalto-1 CubeSat OBC is shown in the figure 3.10. Aatlo-1 CubeSat OBC manages all the on-board activates including payload with the exception of ADCS. The OBC has non-volatile memory to store the scientific and payload data in two predefined packet formats. The spectral imager data is processed using compression algorithm before storing it to the memory. All the uplink and downlink communications are managed by the OBC to transmit and receive the telemetry and telecommand data respectively [34].

The reliability and robustness is very important for the OBC as it manages all the subsystems of the CubaSat, so OBC has redundant design to increase the reliability and life span of the CubeSat. Due to the redundant design, the recovery of OBC subsystem can done by selecting the cold redundant system through the arbiter. The cold redundant system (switched off) consume less

power as compared to hot redundant system (switched on) when power saving has been taken into account. The figure 3.10 shows the Aalto-1 CubeSat OBC design in which two processors along with their RAM and flash memories are placed on the same PCB [34].

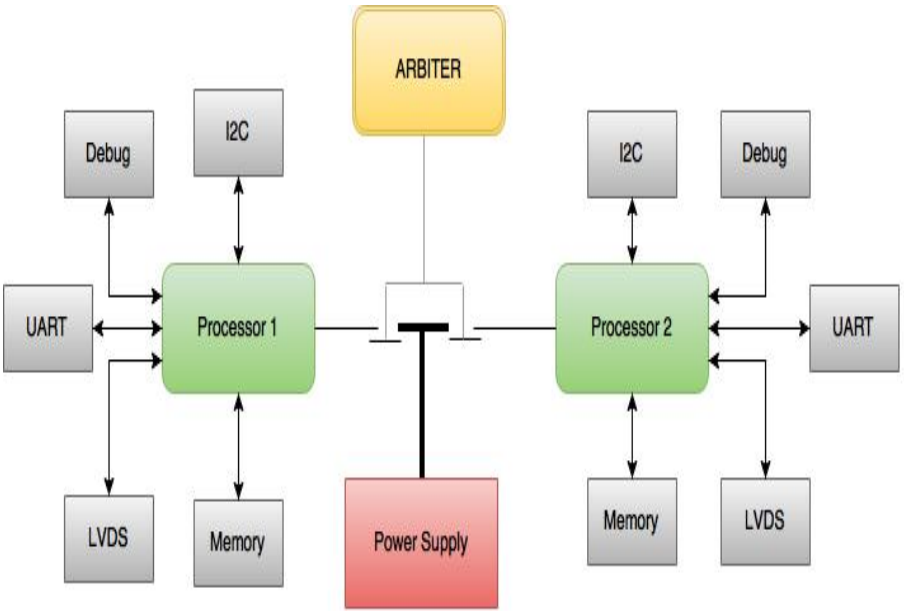

Figure 3.10: High-level block diagram of Aalto-1 CubeSat OBC [34]

The OBC handles all the commands, their validation and distribution to the respective subsystem for the command execution and collection of telemetry data in the predefined packet format.

The standard I^2C bus communication protocol has been implemented for the interfacing with various subsystems with OBC of Aalto-1 CubeSat. The I^2C has two lines; serial clock line (SCL) and serial data line (SDA) which provide the synchronized data transfer over the bus [35]. Aalto-1 OBC works as the master and control the communication of the bus, which simplifies the complexities of the data transfer processes by eliminating the bus arbitration issues.

Aalto-1 CubeSat OBC interfacing with other subsystems is illustrated in the figure 3.11. The I^2C bus provide the main communication link with other subsystems but some of the components require the customized OBC interface dedicated to each of the subsystem for the increased reliability and robustness.

The AaSI generates large amount of imagery data for which OBC is interfaced with AaSI through SPI (Serial Peripheral Interface) and this large data cube is transferred over LVDS (Low-voltage differential signaling) while the AaSI command interface is through I^2C. The OBC send this imagery data to the S-Band transmitter through SPI interface for high data rate transmission. GPS, UHF transceiver and RADMON is interfaced with OBC through UART(Universal asynchronous receiver/transmitter). The RADMON is also interfaced through I^2C bus for the backup communication link [34].

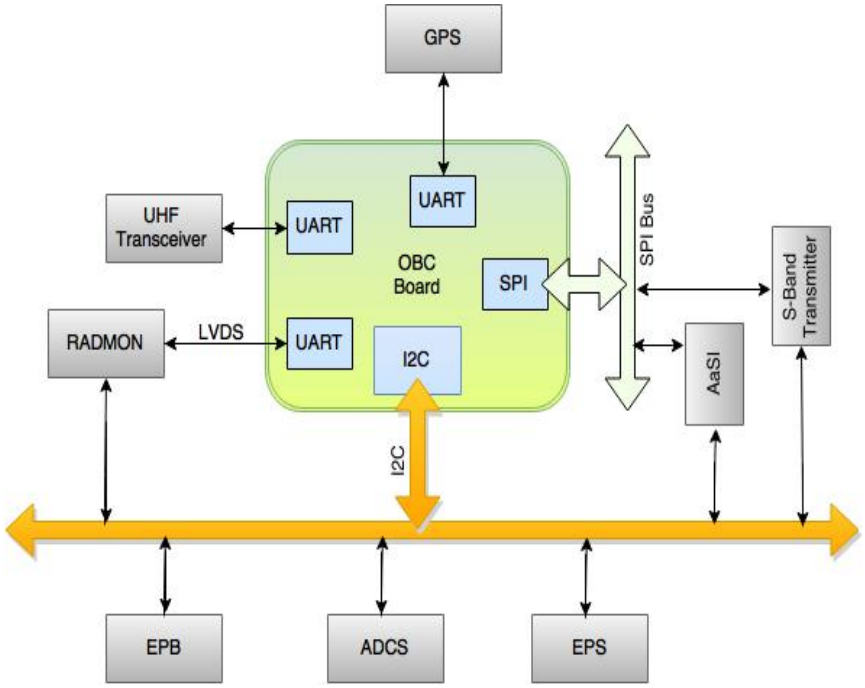

Figure 3.11: Aalto-1 CubeSat OBC interfaces [36]

Telemetry Data Budgeting

Aalto-1 CubeSat OBC collects the data in the predefined format from all the subsystems and send to the ground station when the communication link with ground station is established. An application in the OBC scheduler manage the telemetry data collection process from all the subsystems. The telemetry data is retrieved from each subsystem periodically including the OBC telemetry status data. The collected telemetry data is further processed by health check process and system log is maintained with debug, information and errors [36]. The on-board telemetry data packet format is shown in the figure 3.12 for the data communication protocol. The maximum packet size is 255 bytes. The

telemetry data packet format contains packet length, command field, status, data and checksum and each of the field has specific size as mentioned in the figure 3.12 [37].

Packet Length	Command Field	Status	Data	Checksum
01 byte	01 byte	01 byte	0-253 bytes	01 byte
0-255	0x00-0xFF	0x00-0xFF	Field for additional data	XOR of all bytes in the packet

Figure 3.12: Aalto-1 CubeSat on-board telemetry data packet format

The packet length has one byte of size in which the whole length of the telemetry packet (command, status, data and checksum) is defined which can have value from $0 - 255$ bytes $(0x00 - 0xFF)$. The command field has also the size of one byte which contain the command number that the packet is transmitting while the status filed show the execution status of the command and it has maximum size of one byte. For the successful execution, the value is $0x00$ while $0x01 - 0xFF$ show the respective errors in the signal. Also when OBC send the telemetry packet, the status field is always $0x00$. The data field has maximum size of 253 bytes and it contains the data related to the telemetry packet. The checksum is bitwise XOR of all the bytes in the packet to make sure that packet received has same information without any error. The checksum field has size of one byte. The checksum can be written as in the equation (3.1) [37]

$$checksum = b_1 \; XOR \; b_2 \; XOR \; b_3 \; XOR \; b_4 \; ... \; XOR \; b_n \; . \tag{3.1}$$

Where $b_1 \ldots b_n$ are the telemetry data packet bytes and the complete data packet can be shown in the equation (3.2)

$$data \; packet = |b_1 b_2 b_3 b_4 ... b_n | C|. \tag{3.2}$$

Aalto-1 On-board Scheduler

Aalto-1 OBC perform autonomous execution of task assigned to it as the CubeSat is in LEO and does not have visibility with the ground station all the time. The execution of these assigned tasks are managed through on-board scheduler process. The figure 3.13 illustrates the communication layer architecture of on-board scheduler which is implemented in the Aalto-1 CubeSat mission. The OBC hardware is the physical layer which runs Linux kernel at data link interface with the physical layer, after Linux kernel, on-board scheduler in implemented to control the software task execution on application layer [36].

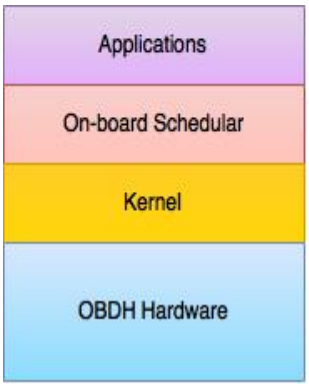

Figure 3.13: Aalto-1 on-board scheduler communication layer architecture

The main objective of scheduler is to perform the software operations required to manage the science mission for the collection of payload data. All the software operations are maintained in the mission control log file which have the information of all the CubeSat operational modes for the whole duration of the mission. The control log file is managed from the ground station through OBC according to the requirements of the mission tasks. These tasks are separate processes running on the application layer of a multitasking operating system, in which each task can be implemented and tested separately [38].

3.2.4 General Design of Aalto-1 Communication system

Aalto-1 communication system has been designed to work in the radio frequency band of UHF and S-band, which have separate radio system modules. The UHF radio frequency channels are used for armature radio and S-band frequency

range is dedicated to the industrial, scientific and medical (ISM) use [39]. The UHF radio system will communicate with ground station at 437 MHz. Due to limited frequency range in UHF, the data rates of UHF transceiver are not high and the omni-directional antennas are used to provide the communication link with the ground station. So UFH radio system has advantage over the other directional antenna radio system as it is very helpful to establish the communication link in case of ADCS failure and when satellite orientation is not known also low frequency signals have marginally less free-space loss as compared to the high frequency signals. Aalto-1 mission require high bandwidth for Payload imagery data transmission, for which S-band (2.42 GHz) frequency is chosen to provide the high data rate link with ground station. The design parameters of Aalto-1 CubeSat radio systems have been discussed in the following section[40].

Aalto-1 Communication in UHF

Aalto-1 CubeSat communication system is using UHF band (437 MHz) radio link for the OBC telemetry, telecommand and beacon signal. The block diagram of Aalto-1 UHF radio system is illustrated in the figure 3.14 in which OBC is interfaced with transceiver through UART. The power amplifier (PA) and low noise amplifier (LNA) are connected thorough RF switches to transmit and receive the signal. The power amplifier is also connected to the power switch to control its operation. The dipole low gain antenna is used for the transmitting and receiving the telemetry and telecommand data respectively [41].

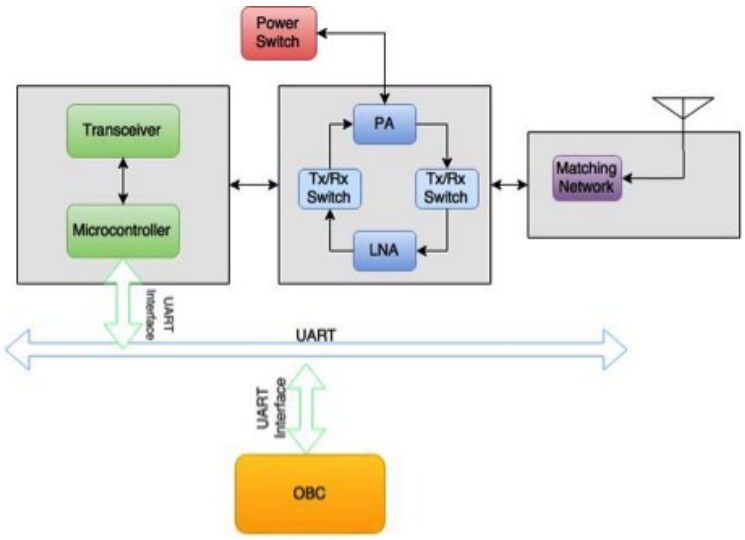

Figure 3.14: Aalto-1 UHF radio communication system for telemetry/telecommand [42]

Parameter	**Value**	**Remarks**
Frequency	437 MHz	Both uplink and downlink
Data rate	9600 *bps*	1200/2400/4800 *bps* slecteable
RF Power	150 mW	22 dBm
Peak Power	1.55 W	
Communication Protocol	AX.25	
Receiver sensitivity	-104 dBm	10^{-5} Bit Error Rate

Table 3.4: Technical specifications of Aalto-1 UHF radio transceiver [41]

Aalto-1 Communication in S-Band

Aalto-1 CubeSat payload has spectral imager which require high bandwidth to transmit the imagery data to the ground station for which S-band radio system is used for the communication downlink [43]. The S-band transmitter with the CubeSat kit bus and additional interface was developed by the Department of Radio Science and Engineering (Aalto ELEC). The technical specifications of Aalto-1 S-band transmitter is given in the table 3.5[44].

Parameter	Value	Remarks
Frequency	2.42 GHz	S-band
Modulation	DQPSK	
Data rate	1.06 $Mbit/s$	
RF output power	500 mW	
Forward Error Correction rate	0.489	Turbo code
Input Voltage	$3.3V$	$3.0V - 5.0\ V$
Current draw	$1.5A$	at 500 mW RF power

Table 3.5: Technical specifications of Aalto-1 S-Band radio transceiver [43]

3.3 Ground Station

Ground station are an integral part of satellite missions as they provide the communication link between the satellite and Earth to meet the objectives of the mission. To establish the continuous link with the satellite multiple ground stations can be established to form a network which can establish the communication link whenever the satellite foot print is available and these ground stations are connected to each other through terrestrial communication links like fiber optics etc. and through these ground stations the telemetry data can be accessed as per requirements [45].

The ground station provide the telemetry, telecommand and tracking facility with the satellite missions through radio links. The ground stations can be used for telecommunication solutions, remote sensing and communication link with space stations as well as with outer space missions for tracking and scientific explorations. These ground stations provide the radio frequency link the various RF band defined by the International Telecommunication Union (ITU)[46].

3.3.1 Aalto-1 Ground Station

Aalto-1 ground station architecture is illustrated in the figure 3.15 in which the CubeSat control room have control terminal computer interfaced with the ICOM-910 radio though serial data converter (CI-V Converter RS232). The control terminal computer is also connected to the Sound IN through analog connection of ICOM-910 radio. 13.8 V DC power supply provide the power to the ICOM-910 radio, rotator driver and CI-V Converter. The ICOM-910 radio is connected to two the two antennas through RF link with the power divider (90° phase shifter). The rotator driver control the SPID RAS rotator for the antenna control as per mission requirement. The table 3.6 shows the Aalto-1 CubeSat ground station parameters for its operations [47].

Location	**Longitude**	**Latitude**	**UHF Freq**	**S-Band Freq**
Aalto Elec, Otakari 5A Espoo Finland	23.830764 E	60.188732 N	437.22 MHz	2.42 GHz

Table 3.6: Aalto-1 CubeSat ground station parameters

The mission control control software is capable of tracking the Aalto-1 CubeSat through Gpredict tracking software solution which can predict the orbital parameter for the CubeSat visibility time window through NORAD TLE and on-board GPS data. Software defined radio is used for the configuration the parameters to establish the communication links. There is in-house telemetry monitoring tool developed for the operations of the CubeSat mission.

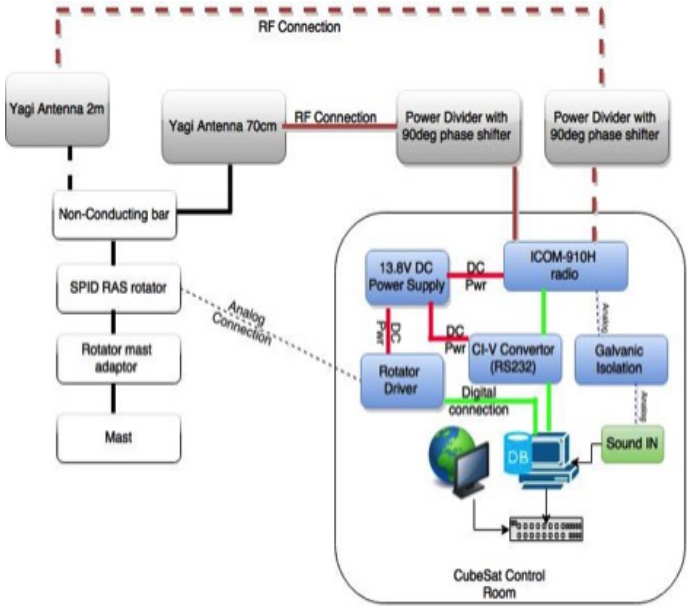

Figure 3.15: Aalto-1 CubeSat ground station architecture [47]

Chapter 4

Aalto-1 CubeSat Mission Managment

4.1 Aalto-1 CubeSat Mission Management Strategy

Aalto-1 CubeSat mission is divided into three main mission phases, LEOP, service phase and de-orbit phase respectively for their in-orbit operations as shown in the figure 4.1. The service phase is further categorized into three operational phases which are AaSI operations, RADMON operations and communication phase. The de-orbit phase is also further categorized into EPB experimentation and de-orbiting operations.

Figure 4.1: Aalto-1 CubeSat in-orbit mission phases

4.1.1 Aalto-1 CubeSat Power Management

Aalto-1 CubeSat mission power management strategies during the various phases of it's in-orbit operations are described in following sections.

Power Management during LEOP

After the deployment of Aalto-1 CubeSat in the orbit by launch vehicle, ADS (antenna deployment system) is switched on to deploy the UHF antennas for the establishment of communication link with the ground. During this operation, the OBC and UHF communication modules are on while the other subsystems (Payloads, GPS, S-Band communication module and ADCS) are switched off. When the UHF antennas are deployed, the ADS and OBC are switched off. So, during the initial phase of LEOP, 7 W of peak power is used for 60 seconds by ADS for antenna deployment. After the successful deployment of UHF antennas, in-orbit testing (IOT) is performed to check the health status of each subsystem of the CubeSat.

Power Management during Service Phase

After the successful health check of the satellite in IOT, the routine operation of the CubeSat is performed in the service phase. The service phase is further categorized in three phases: Spectrometer phase, RADMON phase and communication phase, these categories help to manage the payload operations so that power can be utilized optimally. In the spectrometer phase, a command is sent from the ground station to take the imagery data of the desired location at specific time. Spectrometer also communicate with ADCS for the orientation of satellite and GPS data for the Geo tagging of imagery data. So, when AaSI is in the operational mode, ADCS and GPS data is needed to perform the required tasks. The estimated power required to perform AaSI operation is 6.48 W as shown in the table 4.1

Subsystem	**Standby power**	**Peak Power**
AaSI	0 W	4 W
ADCS	0.5 W	1.8 W
GPS (active antenna & receiver)	0.045 W	0.13 W
OBC	0.25 W	0.55 W
Total Power	0.795 W	6.48 W

Table 4.1: Estimated power required for AaSI operations

When science mission data related to radiation monitoring is required, Aalto-1 CubeSat operational mode is changed to RADMON phase. In this phase the spectrometer and GPS are turned off while ADCS and OBC perform their normal operations as RADMON acquire the data from ADCS for the orientation of the satellite and from OBC for time and date stamping to record the electron, proton fluxes and magnetic field data. The power budget required for the RADMON operation is 5.4 W as shown in the table 4.2

Subsystem	**Standby power**	**Peak Power**
RADMON	0W	1.5 W
ADCS	0.5 W	1.8 W
UHF communication module	0.2 W	1.55 W
OBC	0.25 W	0.55 W
Total Power	0.795 W	5.40 W

Table 4.2: Estimated power required for RADMON operations

When the Aalto-1 CubeSat is in the visibility of the ground station, the operational mode is switched to the communication phase. The ground station visibility predictions can be calculated based on the orbital position of the satellite. During communication phase, UHF communication module and S-band transmitter module is switched on, so that OBC can send telemetry and imagery data to ground station when the communication link is established. The estimated power required during the communication phase is 7.4 W as shown in the table 4.3

Subsystem	**Standby power**	**Peak Power**
S-Band transmitter	0 W	3.5 W
ADCS	0.5 W	1.8 W
UHF communication module	0.2 W	1.55 W
OBC	0.25 W	0.55 W
Total Power	0.95 W	7.40 W

Table 4.3: Estimated power required during communication phase

During the communication phase, when there is no imagery data to be transmitted from the CubeSat, the S-band transmitter can be switched off and RADMON can be switched on during the communication phase.

Power Management during De-orbit Phase

The service life of Aalto-1 CubeSat is two years and in the last phase of Aalto-1 CubeSat mission, electrostatic plasma brake (EPB) experimentation will be tested. As EPB experimentation change the orbit of CubeSat so this electric sailing concept [18] experiments will be performed during the de-orbit phase of the satellite. For this scientific experiment, EPB tether is deployed at different lengths, after which it is electro-statically charged either positive or negative and the orbital changes will be monitored using ADCS and GPS data. The estimated power budget required for EPB experimentation is 7.03 W as shown in the table 4.4

Subsystem	**Standby power**	**Peak Power**
Electrostatic Plasma Brake	2.3 W	3 W
ADCS	0.5 W	1.8 W
UHF communication module	0.2 W	1.55 W
OBC	0.25 W	0.55 W
GPS	0.045 W	0.13 W
Total Power	3.295 W	7.03 W

Table 4.4: Estimated power required during electrostatic plasma brake experimentation

When the plasma brake experimentations are complete, all the subsystems of CubeSat are turned off including the communication modules so that the frequency does not cause the interference with other satellites.

4.1.2 Aalto-1 CubeSat Data Management

As Aalto-1 CubeSat is multi objective mission having three different payloads for the scientific experimentation and remote sensing and these payloads have different interfaces with the OBC through I^2C UART and SPI to send the commands and telemetry data. The OBC software provide the support to communicate through these interfaces and an abstraction layer between the hardware and software level. The payloads communication is of two types, containing science mission data and telemetry data for which two different approaches are implemented. In the first approach, the telemetry data is collected and stored to the memory as per requirement of each payload while in the second approach the subsystems interact with the payload to achieve the required goals for example spectral imager require the ADCS information to perform the operation at the right position [36].

OBC Data Communication with AaSI

The OBC sends the command data to AaSI through I^2C bus while AaSI use the SPI bus to send the imagery raw data (16-bit words) using the OBC serial clock signal (SCK). OBC process the raw data with compression algorithm and store to the non-volatile memory. When the ground station link is established through S-band, the stored data is transmitted to the ground in a fixed predefined 64 bytes length frame [37].

OBC Data Communication with RADMON

Aalto-1 CubeSat OBC has interfacing with RADMON payload through UART over Low-voltage Differential Signaling (LVDS) and I^2C. RADMON perform the scientific measurements of proton and electron fluxes along with the date,

time, CubeSat position, relative orientation of RADMON and magnetic field data for the radiation experimentation in the orbit. The RADMON payload sends the scientific data through UART over LVDS to OBC. RADMON also collects the data from ADCS for the orientation and time/date data from OBC. The I^2C bus interface is used for backup communication in-case UART failure. RADMON provide the scientific mission data whenever it's possible during the service phase of the mission with some exceptions (when Spectrometer is in use and while communications with ground) [36].

OBC Data Communication with EPB

The plasma brake experimentations will be performed in the last phase of Aalto-1 CubeSat mission. This scientific experimentation has sequence to small operations to test the concept of electric sailing [24]. Aalto-1 OBC ensures theses scheduled operations as per plan, sent from the ground station. The telemetry data will collect the tether length along with the currents, temperatures and positional data. OBC communicate with plasma brake payload through I^2C bus protocol[38].

4.1.3 Aalto-1 CubeSat Communication Management

Sat Master Pro software tool is used for the link budgeting analysis of GS communication. The tool is developed by Arrowe and helps to compute and analyze the data budgets and link budgets for the communications[48]. Aalto-1 CubeSat link budgets and various parameters have been analyzed for the performance evaluation of Aalto-1 communication system.

The ratio of energy per bit to the spectral noise density (Eb/No) is the measure of signal to noise ratio which is the receiver measurement for the signal strength. The figure 4.2 shows the plot of Eb/No vs the bit error rate. The plot illustrates the digital link performance to assess the communication links [49]. The logarithmic plot is estimated using Sat Master Pro software and it shows

the decreasing trend of Eb/No with the decrease in the bit error rate (BER) for the uncoded coherent QPSK modulation scheme.

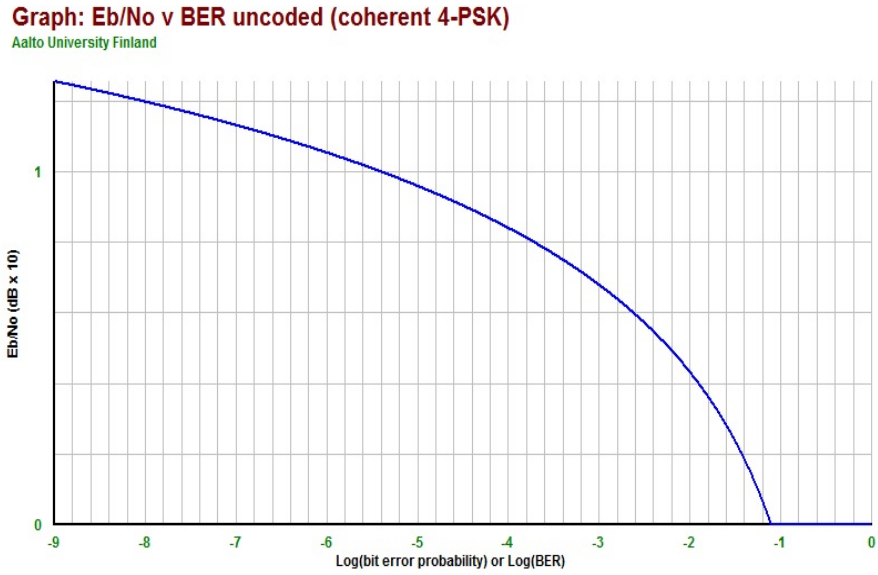

Figure 4.2: Eb/No vs bit error rate plot for uncoded coherent 4-PSK

The tabulated comparison of digital modulation schemes shown in the figure 4.3 is generated from the Sat Master Pro tool [48]. The comparison analysis of various modulation schemes is performed with reference to the Eb/No and bandwidth efficiencies. The Eb/No values used in the table are uncoded modulation schemes. The bandwidth efficiencies are measured in bits/sec/Hz. The binary phase shift keying (BPSK) has the lowest values of Eb/No and bandwidth efficiency as compared to QPSK which has the same value of Eb/No but double the bandwidth efficiency.

Comparison of Digital Modulation Schemes
Aalto University Finland

Log(BER) = -7

Notes
Eb/No values shown do not include channel coding
Bandwidth efficiencies, BW(eff), shown in bits/sec/Hz

Modulation	Eb/No(dB)	BW(eff)
BPSK	11.31	1.00
4-PSK	11.31	2.00
8-PSK	14.75	3.00
16-PSK	19.26	4.00
32-PSK	24.20	5.00
64-PSK	29.36	6.00
128-PSK	34.65	7.00
256-PSK	40.00	8.00
4-QAM	11.31	2.00
16-QAM	15.20	4.00
64-QAM	19.59	6.00
256-QAM	24.34	8.00
1024-QAM	29.34	10.00
4096-QAM	34.52	12.00

Figure 4.3: Comparison of digital modulation schemes for Eb/No and bandwidth efficiencies

4.1.4 Ground Visibility Time per Orbit

In LEO and MEO, satellites can not communicate with the ground station all the time because it has some specific visibility window to communicate during an orbital period. The satellite visibility time window can be predicted using its orbital parameters. The figure 4.4 shows the graphical interface of real-time satellite tracking and orbit prediction tool which can estimate the time of next satellite pass with respect to ground station. This tool uses the NORAD TLE data to predict the satellite orbits for ground station visibility [50].

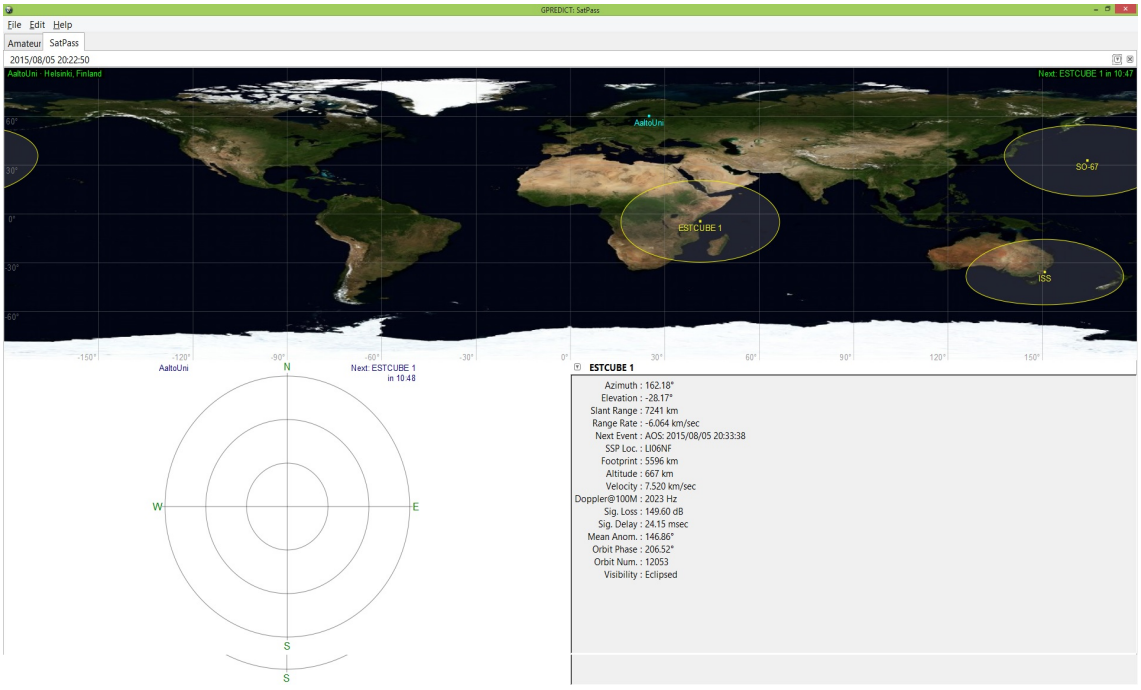

Figure 4.4: Orbital prediction tool (Gpredict) for the prediction of satellite passes using on-line NORAD TLE updates

Telemetry and Telecommand Data Links

For Aalto-1 CubeSat telemetry and telecommand operations, radio link will be established depending upon the foot print availability for the ground station using transceiver at 437 MHz. The transceiver can be configured to maximum of 9.6 $Kbit/s$ along with the 1.2/2.4/4.8 $Kbit/s$ configuration options which can easily fulfill the Aalto-1 mission requirements for telemetry and telecommand operations. Based on these data link configuration, input voltage range (6.5 $V-$ 12.5 V) with 1.55 W peak power can be selected [41]. For data optimization different modulation schemes Binary Phase Shift Keying (BPSK), Frequency Shift Keying (FSK) and Audio Frequency Shift Keying (AFSK) can be selected as per requirements. These simple modulations schemes provide the robust and reliable implementation of communication data links. The receiver has the sensitivity of -104 dBm at 10^{-5} bit error rate [41].

S-Band Secondary Downlink

As Aalto-1 payload AaSI require high data rate for the transmission of imagery data to ground station which can be configured to 1.06 $Mbit/s$ with DQPSK modulation scheme. For the reliable and robust link, directive antenna are required with the high gain in S-band communication link. The power requirements are also high for S-band radio system transmission as compared to the UHF radio system [44].

4.2 Aalto-1 CubeSat Orbit Simulations

Systems tool kit (STK) software is used for the modeling and simulations of satellites to analyze the dynamic behavior of satellites in space. Aalto-1 CubeSat mission was inserted as model along with its mission requirements. The orbital simulations were performed to analyze the mission and observe the change in various parameters to evaluate the performance of the CubeSat. The figure 4.5 illustrates the orbital simulation results of Aalto-1 CubeSat over the Earth model. Otaniemi area in Espoo Finland is selected as the ground station. The orbital path in displayed as red in the figure 4.5. The simulation results can also predict the next pass for the ground station communication.

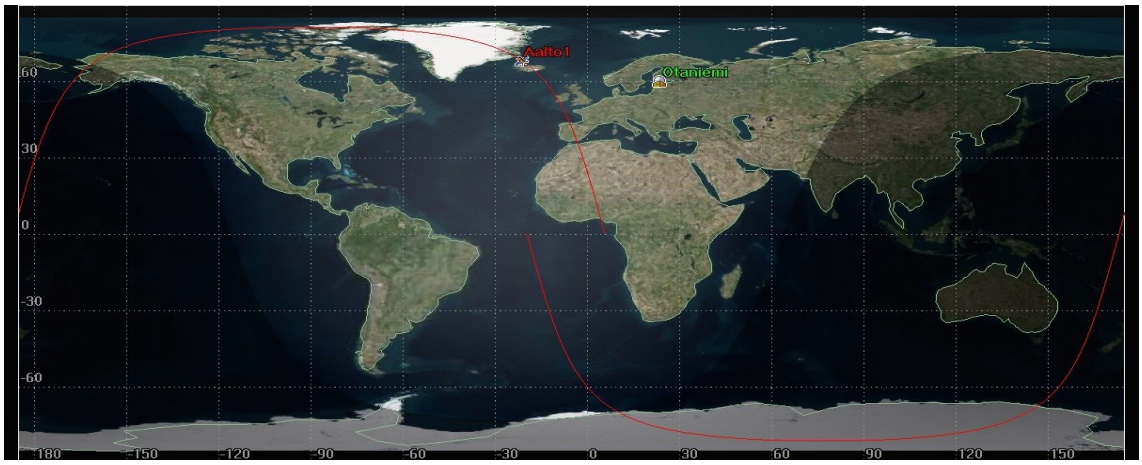

Figure 4.5: Aalto-1 CubeSat mission orbital simulation with STK

The figure 4.6 shows the simulation plot of Euler angles for the orientation analysis of Aalto-1 CubeSat mission. The change in the 3-dimensional orientation

of CubeSat show the dynamic behavior in the space environment.

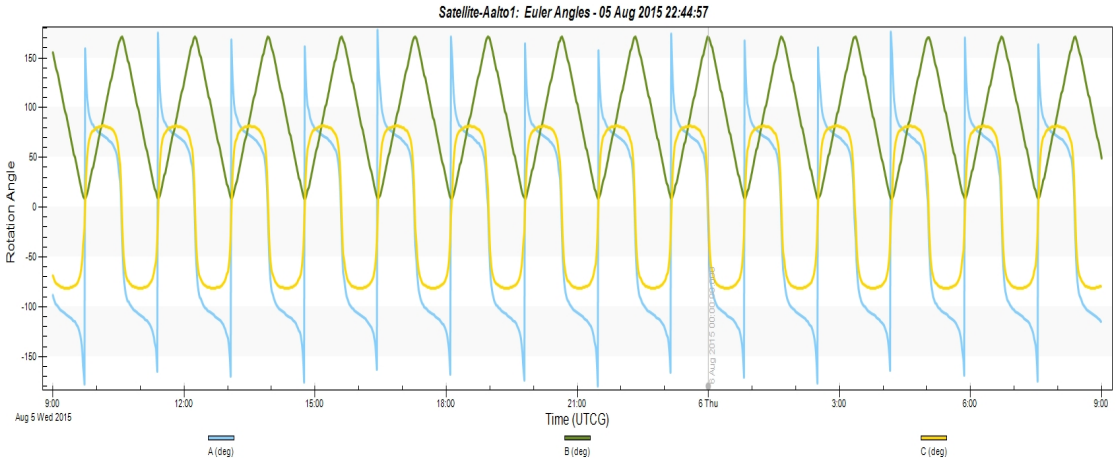

Figure 4.6: Aalto-1 CubeSat mission model for Euler angles

The figure 4.7 displays the simulation results of β angle which show the angle between orbit plane and sun direction. The β angle helps to compute the eclipse time of the satellite during an orbital period. The simulation results show the change of β angle from 22.7° to 21.9° within the span of one day.

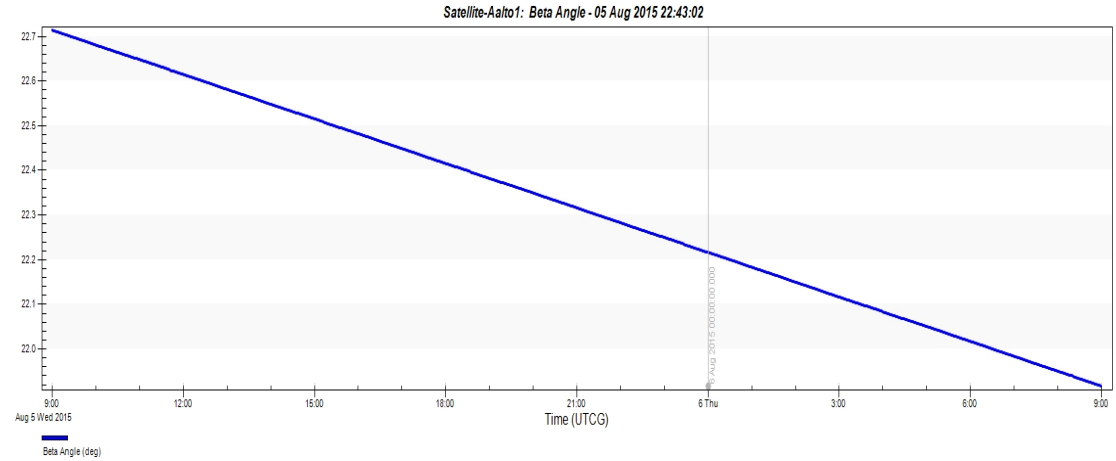

Figure 4.7: Aalto-1 CubeSat change in angle between orbit plane and sun direction according to STK simulation

The figure 4.8 illustrates the Eclipse time slots of Aalto-1 CubeSat mission using STK simulations. The plot shows the various eclipse timings highlighted in the graph for simulated orbital parameters of Aalto-1 CubeSat.

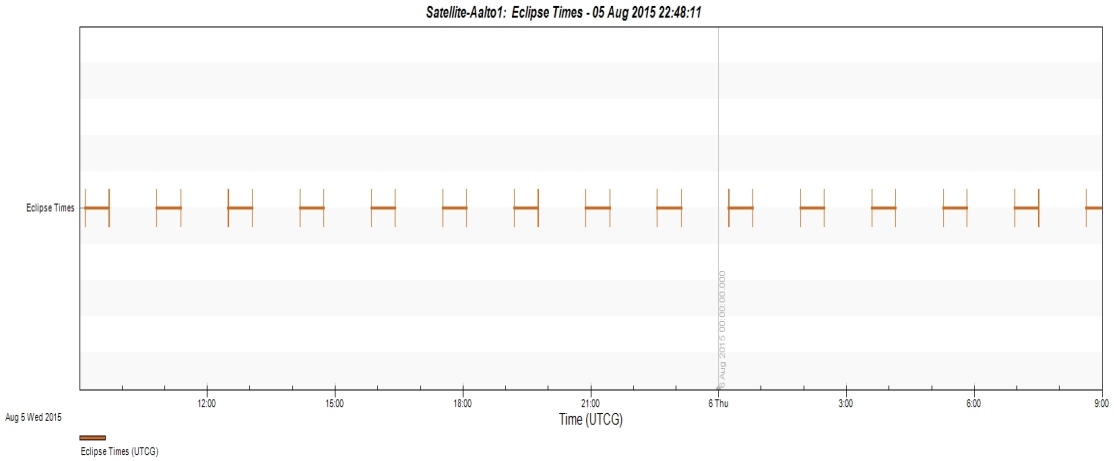

Figure 4.8: Eclipse time plots of Aalto-1 CubeSat according to STK simulations

Chapter 5

Small Satellite Mission Simulations and Results

5.1 Simulations of Mission Schedule and Budgets

In this section, the GA simulation results are discussed in details and satellite mission scheduling problem solving techniques using constraint based approach has been explained. A comparison analysis of these two mission scheduling techniques has also been included.

5.1.1 Simulation Results of Genetic Algorithm

The genetic algorithm has been simulated in the Matlab for the satellite scheduling and optimization of multi-objective missions. Matlab optimization tool as shown in the figure 5.1 has been used for GA in which the fitness function has been generated using the equation as described in the chapter 2. The six variables have been used for constraint dependent simulation results. As Aalto-1 CubeSat has not been launched yet so for the simulations of GA following tabulated values have been used for the simple mission scenario as shown in the table 5.1

Mission	Position		Time Window	Priority	Memory	Power	Weather
	Lat	Long					
1	22.36	-112.56	1	3	300	20	15
2	46.87	-88.23	4	5	50	35	10
3	67.21	-121.14	7	1	200	40	60

Table 5.1: Mission scenario for GA simulations

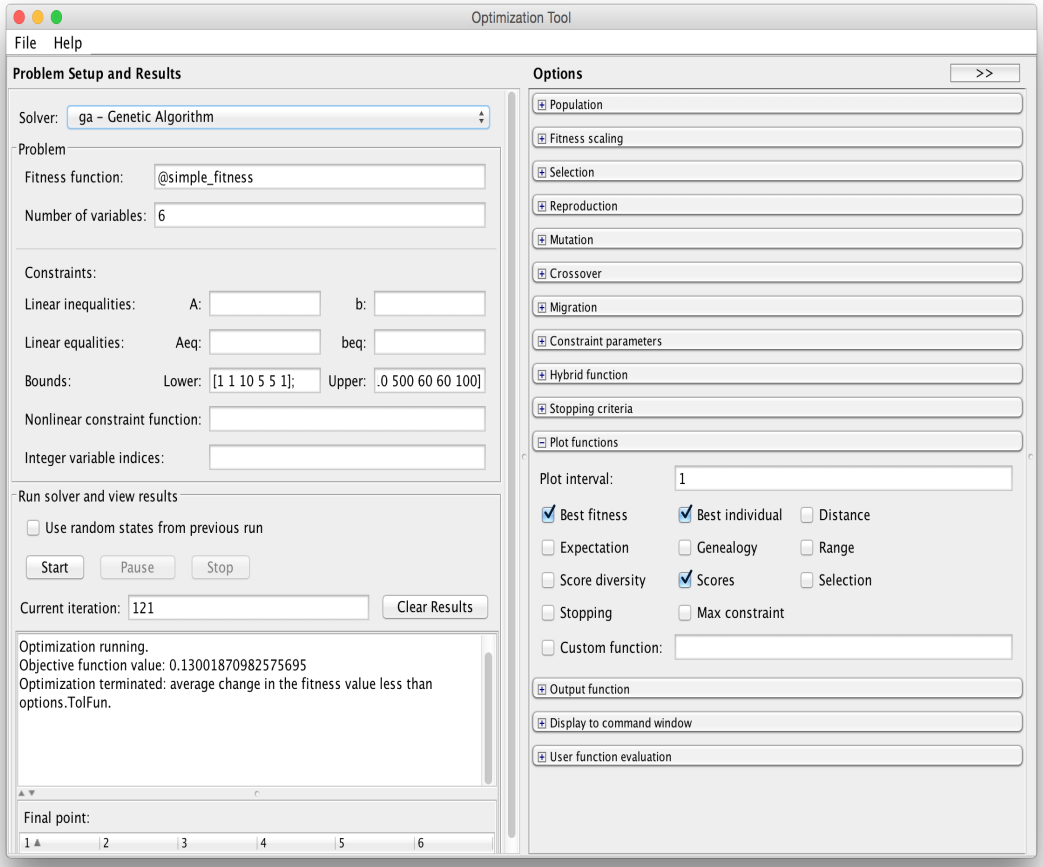

Figure 5.1: Genetic Algorithm Matlab toolbox overview

The genetic algorithm takes the initial population data and optimize iteratively the population for individual solutions based on the constraint dependent function. GA selects random individual from the population and generate the children for next generation and ultimately produce the optimized solution using the mutation technique [15].

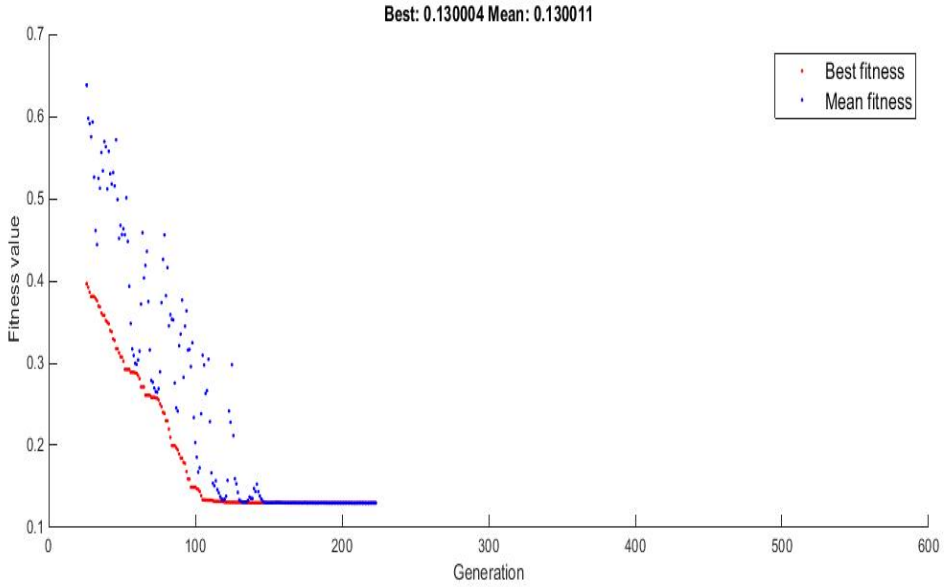

Figure 5.2: Genetic Algorithm simulation for fitness function best score optimization

The figure 5.2 shows the optimized values of fitness function which are minimized using the crossover technique iteratively. In this technique two parent individuals are selected randomly to produce the children for next generation until the fitness function is optimized to the best results. The figure 5.2 shows that fitness function is optimized in 230 iterations to obtain the best fitness value. The mean value of fitness function decreases when it has crossover with the best individual and iteratively crossover of these individuals with the best individual cause the optimized fitness function. It can be observed in the plot 5.2, that the mean value starts decreasing with the repetition of crossover and reaches best fitness function after almost 150 iterations. During the initial stage of optimization, the fitness function values are improved quickly from the early population size but when the fitness function values are close to the optimal value during the later generations, the process of optimization become slow to improve the fitness function until the optimized point reached. As the plot 5.2 illustrates that initially the best fitness and mean fitness values were 0.4 and 0.65 respectively and these value are optimized rapidly during 100 iterations and later on the process was slowed until the best fitness and mean fitness values reached 0.13 respectively [15].

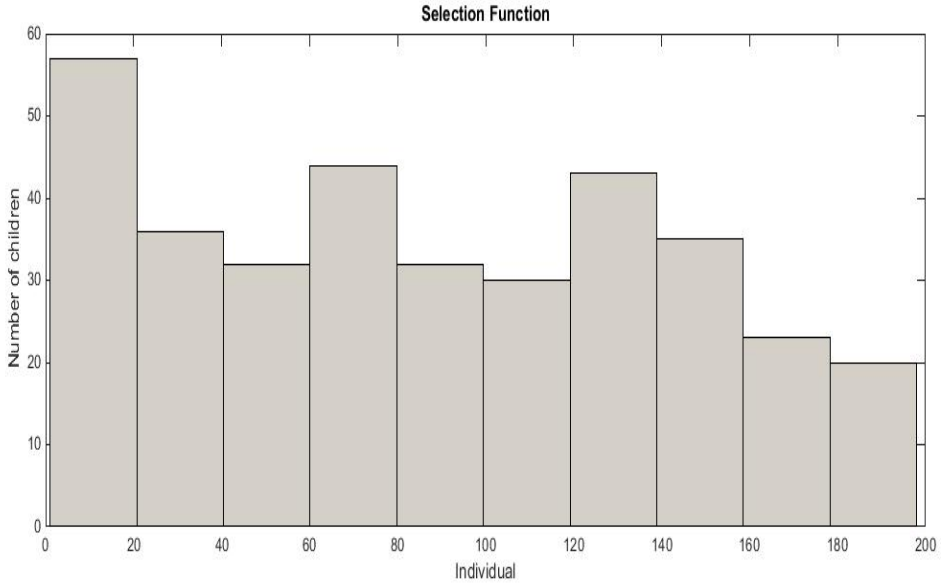

Figure 5.3: Genetic Algorithm simulation results for selection function

The figure 5.3 shows the selection function plot, in which x-axis show the individuals and y-axis show the number of children produced. The selection function compute the values in equal steps where parents are selected within the step. The individuals are selected randomly from the population and produce the children contributing to the next generation using the scaled values of fitness function. During the selection process an individual can be selected again as parent to generate more children which contribute its genes to more children [15].

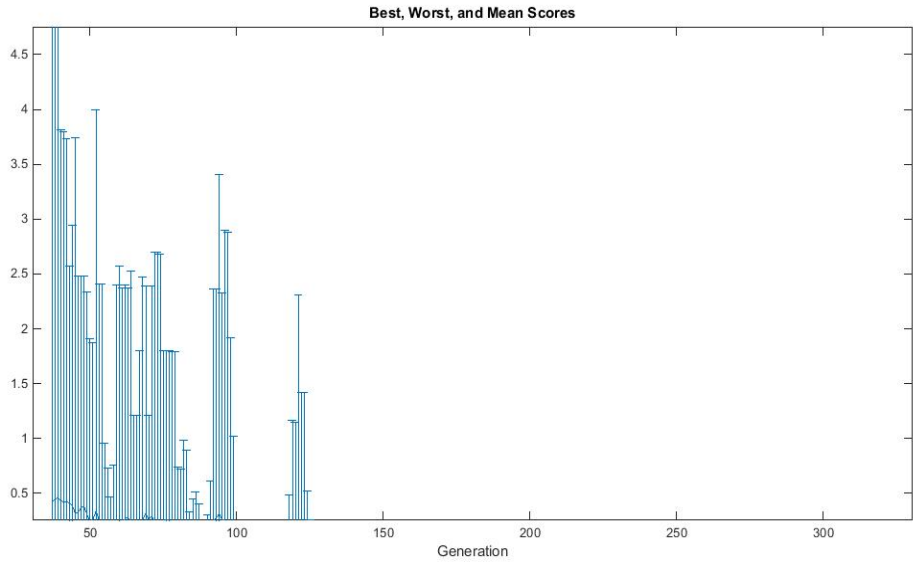

Figure 5.4: Genetic Algorithm simulation results for the fitness function diversity score

The figure 5.4 shows the best, worst and mean score of fitness function during the GA optimization. The x-axis show the generation while the y-axis show the fitness functions values. In the beginning of plot, the values are high because of mutation in which random individuals change from parents to children that increase the diversity values. With the iterative optimization of fitness function, the diversity decreases reducing the amount of mutations [15].

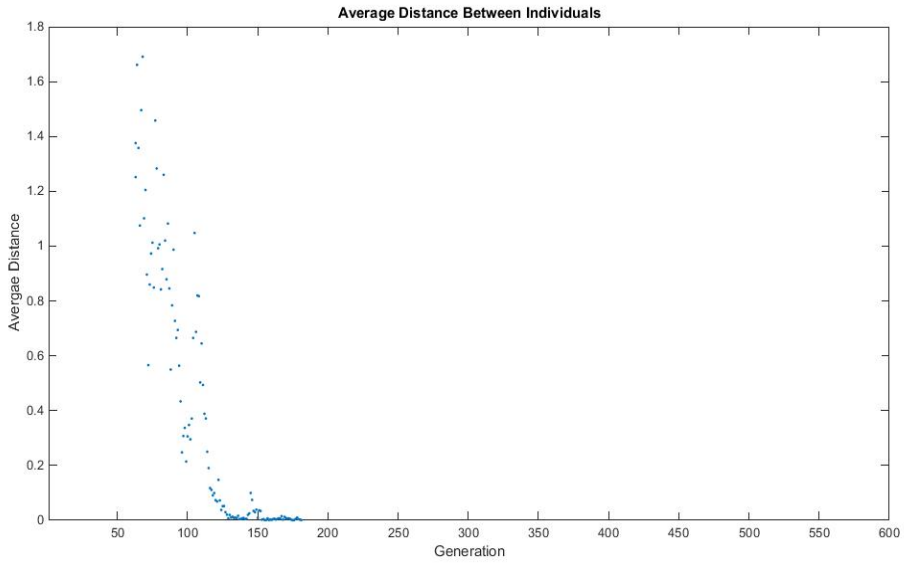

Figure 5.5: Genetic Algorithm simulation results for average distance b/w individuals

The figure 5.5 illustrates the average distance between the individual which show the diversity of the GA. The diversity of the GA is the key factor to analyze the performance of the algorithm because when the distance between the individual is high the diversity is also high similarly when average distance between individual is low, the diversity is low as well. GA does not perform well when the diversity values are high causing starting and error issues. The random change of individual parents to form children effect the diversity of GA. The figure 5.5 shows the generation on x-axis and average distance between the individuals on y-axis. In the simulated results, initially the diversity was high but its value decreased with the number of iterations and after 130 iterations, the diversity value is low as it reaches close to the optimal solution [15].

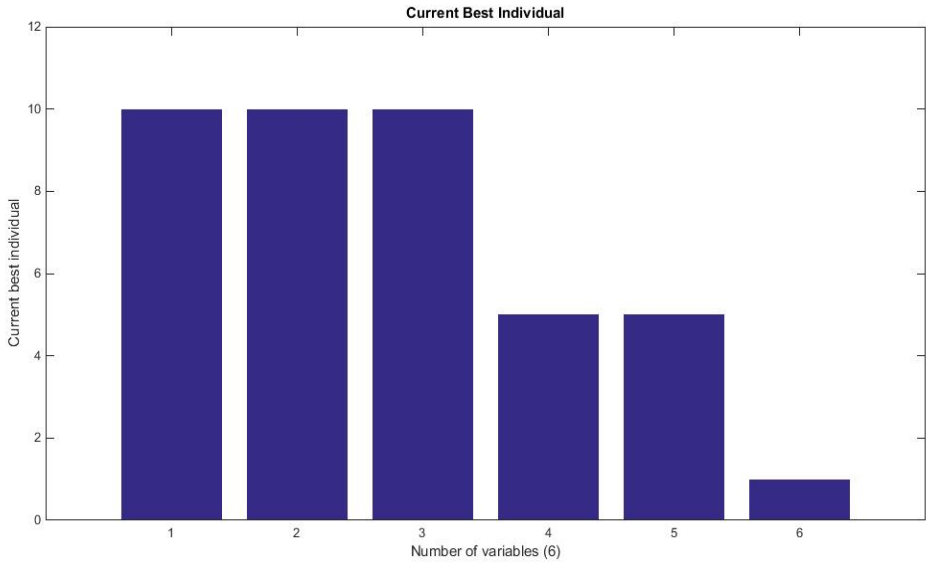

Figure 5.6: Genetic Algorithm simulation results for selection of best individual

The figure 5.6 shows the current best individual selection of variables. The x-axis show the number of variable and y-axis show the current individual score. In figure 5.6, the first three variables are selected as best ones, having same current best individual score. In the problem modeling for the GA, the first three variables are defined as memory size, power and time window respectively. So the scheduling operations can performed as per selection of current best individual tasks. For the simulation results, constrained minimization techniques has been used while tournament method is used for the selection of operator. The GA is very efficient approach to solve the complex multi-objective satellite scheduling problems as it can easily optimize many scheduling tasks within short interval of time resolving all the constraint dependent issues [15].

5.1.2 Modeling of Constraint based Satellite Scheduling and Planning

In the constraint based scheduling approach, the figure 5.7 shows the satellite scheduling and planning CSP model in which Two CSP solver modules are used to schedule the tasks depending upon their constraints. In the first CSP solver, subsystems operations are used as variable in the task domain while

the constraints are number of tasks to be performed and their priority. The CSP solver tabulate these tasks in the subsystems and tasks which are used by the second CSP solver in which tasks are defined as variables in time domain whereas, time preference and tasks correlations are used as constraints to model the final scheduling table that contains information regarding the tasks to be performed and their time slot of operation [51].

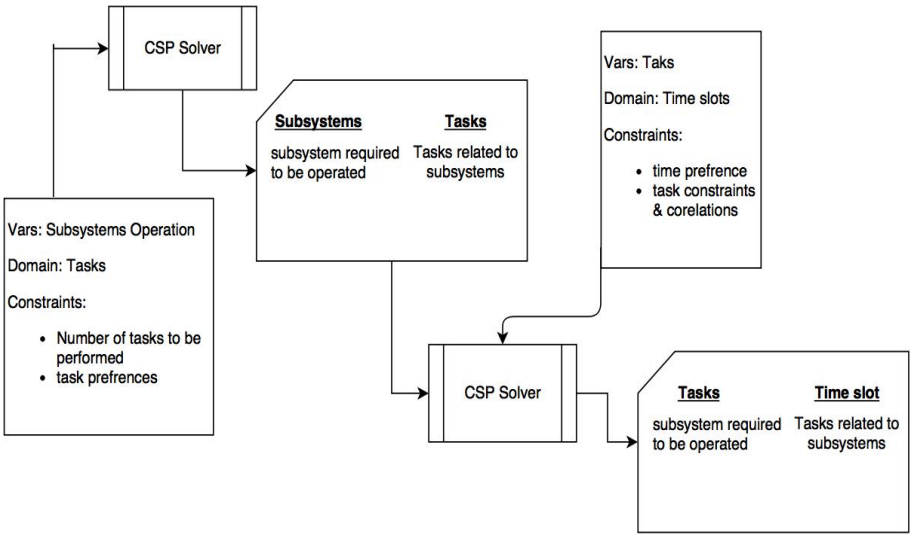

Figure 5.7: CSP based modeling of satellite scheduling and planning

Comparing the both scheduling and mission planning techniques, the GA has advantage over the CSP based scheduling technique because GA can handle the complex task management with the efficient and reliable solution as it generates selections of tasks based on its best fitness function iteratively. While CSP based scheduling is viable solution for simple satellite operations without any complexities and simple scheduling can be optimized using the constraints and variables in the task domain. When the tasks of multi-objective mission are more complex, the GA optimization techniques is preferred over the CSP because GA is more efficient to handle complex tasks within the short span of time.

5.2 Satellite Mission Planning Tool

The satellite mission planning tool is developed to calculate the power budgets according to different subsystems requirements for performing the operations

based on the current orbit of satellite which is calculated using TLE. Similarly, communication and data budgeting calculations can also be performed using this tool to optimize the scheduling tasks. The figure 5.8 illustrates the satellite mission planning tool GUI interface which is developed in the Matlab guide. The tool is divided into different panels: Orbital parameters, subsystems power requirements, power budgets, and ground station parameters to compute the communication and data budgets. The tool provides the support for various configurations and managing the operational tasks.

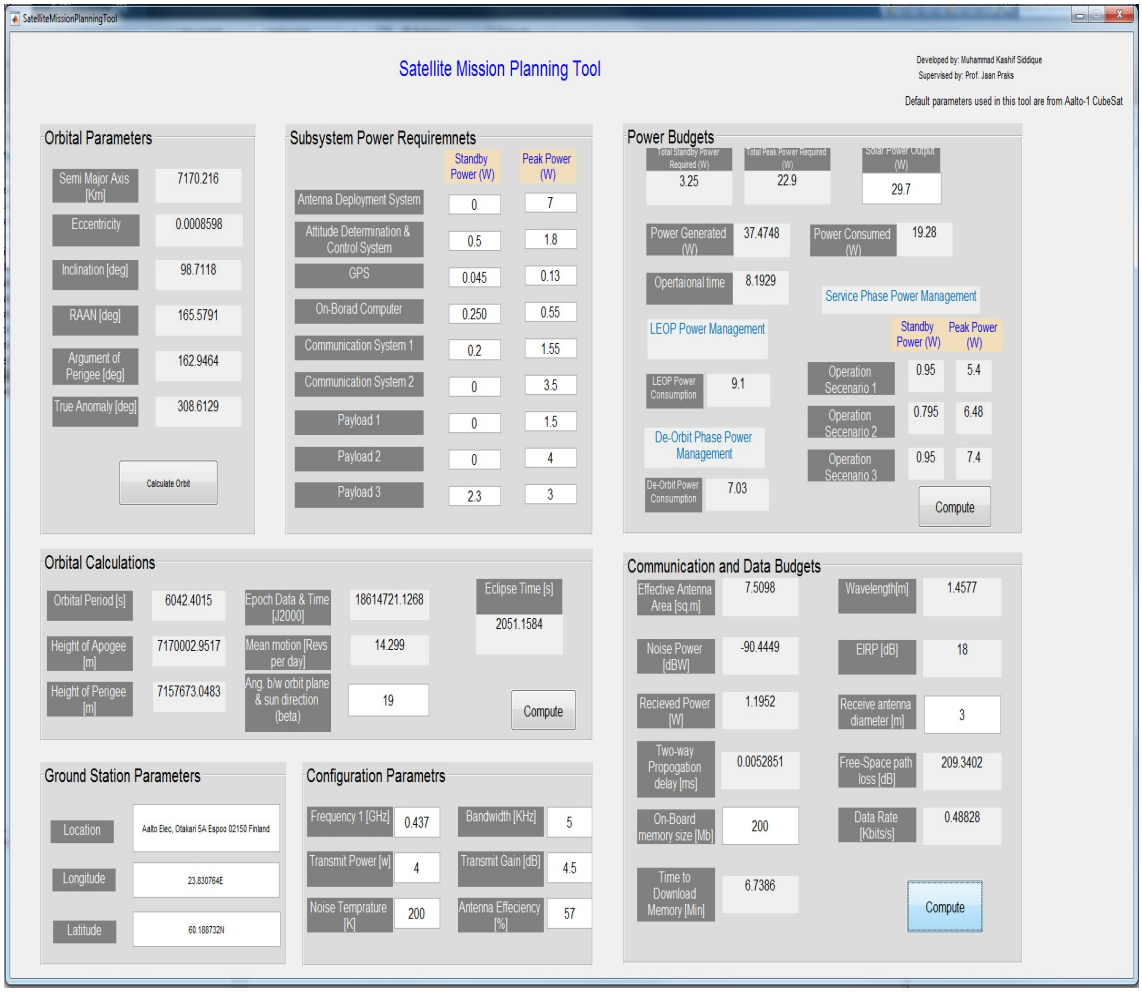

Figure 5.8: Graphical user interface of satellite mission planning tool

Orbital Calculations

The orbital calculation module uses the TLE file, downloaded from the NORAD web. The TLE parameters are incorporated in the tool to calculate the Keplerian elements (semi-major axis, eccentricity, inclination, RAAN, argument of

perigee and true anomaly). The Keplerian elements are further used to compute the orbital period, perigee, apogee, mean motion and angle between orbit plane and sun direction β. The β angle is used to calculate the eclipse time during the orbit. The figure 5.9 shows the satellite planing tool orbital calculations, in which EYESAT-1 CubeSat TLE is used to calculate the orbital parameters.

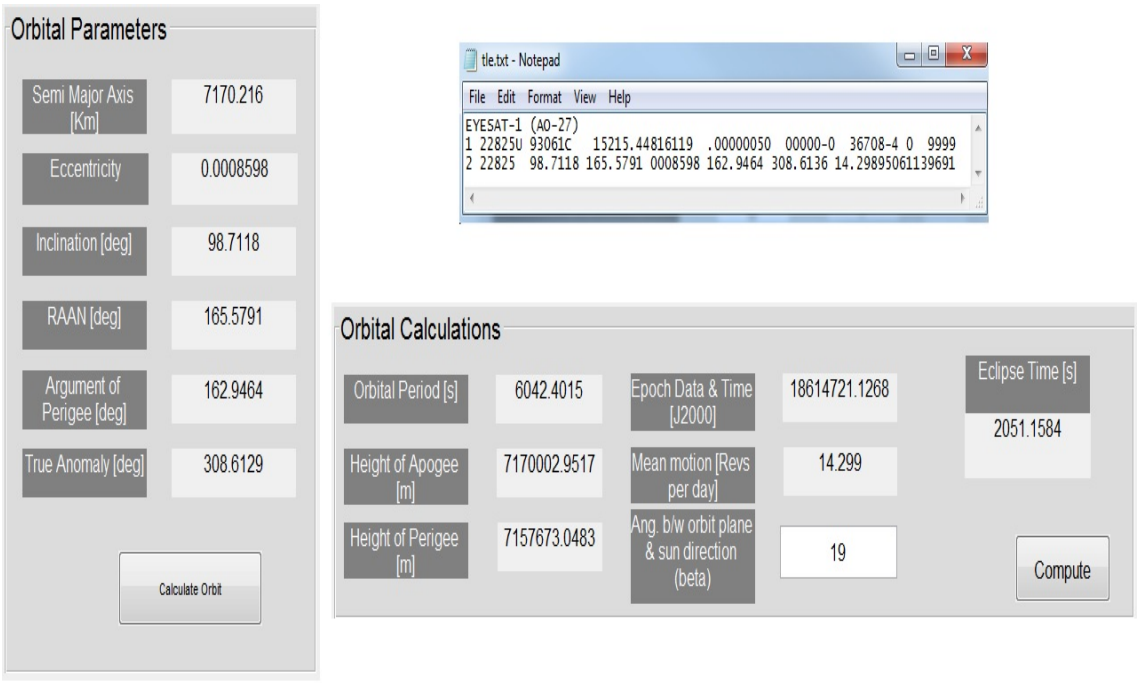

Figure 5.9: Orbital computation module of the satellite mission planning tool

Power Budget Calculations

Power utilization and it's management is important during all the satellite mission phases. Satellite subsystems required to be moderated for power consumption for the successful mission performance because some task require more power than others depending upon the time of operation and power requirement for the specific unit. A satellite mission should never fail due to the mismanagement of power budget for which fool proof measures can be incorporated into the satellite design to avoid the anomalies [52].

The orbit average power (OAP) is an important factor to figure out that how much power is available per orbit and how much power can be utilized during the orbit for the satellite operation. Generally the OAP is 60% of power from solar panel[52].

The power produced during single orbit can be calculated using the solar panel output (SP_{out}) and the orbital period (τ)of the satellite. The power generated ($Pwr_{produced}$) during the orbital period can be calculated by the equation 5.1[53]

$$Pwr_{produced} = SP_{out} \times \tau. \tag{5.1}$$

The power generation can be calculated by the equation 5.2 when there is an eclipse period ($t_{eclipse}$) during the single orbit [53]

$$Pwr_{produced} = SP_{out} \times (\tau - t_{eclipse}), \tag{5.2}$$

while the eclipse period($t_{eclipse}$) can be calculated by the equation 5.3[54]

$$t_{eclipse} = \{\cos^{-1} \frac{\sqrt{(1 - R^2)}}{\cos \beta}\} \frac{\tau}{\pi}. \tag{5.3}$$

In the equation 5.3, R is the radius of Earth, β is the angle between sun-orbit-plane and τ is the orbital time period of the satellite.

From the previous equations, the available operational time t_{op} during the single orbit can be estimated in the equation 5.4[53]

$$t_{op} = \frac{Pwr_{produced} + \tau \times Pwr_{stored}}{Pwr_{stored} - Pwr_{consumed}}, \tag{5.4}$$

where Pwr_{stored} is the power stored in the batteries and $Pwr_{consumed}$ is the power utilized by different subsystems.
As every satellite subsystem has different power requirements and based on that different modes of power can be configured. So the operational time calculations can be generalized by using these different power modes as shown in 5.5. For example, GPS power mode is switched to energy saving mode during last two orbits, the new GPS power mode require the calculation of operational time t_{op} based on the previous consumption of power during previous orbits. So the operational time can be estimated by considering the n number of power modes as shown in the generalized equation for estimation of operational time [53]

$$t_{op} = \frac{Pwr_{produced} + Pwr_{stored}(\tau + t_1 + t_2 + ... + t_n) + P_1t_1 + P_2t_2 + ... + P_nt_n}{Pwr_{stored} - Pwr_{consumed}}. \tag{5.5}$$

In the equation 5.5, P_n and t_n are denoted for power modes and operational time during orbital periods for n number of power mode and n number of orbits, respectively. For the estimation of maximum operational time t_{maxop} for some specific power mode during the mission requirement, the generalized equation 5.6 can be used. In the equation, for maximized operation time t_{maxop} all the power modes are held at constant operation time except for one power mode. For example, when the mission require some specific operational time during a single orbit then that specific time is set constant for different power modes (e.g. OBC overpower mode and communication overpowered mode) for the estimation of maximum operational time where P_A and P_B refer to the maximum consumption of power and donated power form other subsystems respectively, as shown in the equation 5.6 [53]

$$t_{maxop} = \frac{Pwr_{produced} + Pwr_B(\tau + t_1 + t_2 + ... + t_n) + P_1t_1 + P_2t_2 + ... + P_nt_n}{Pwr_B - Pwr_A}. \tag{5.6}$$

For the calculations of battery storage capacity $Bat_{capacity}$, the depth of discharge (DoD), number of battery cells used N_c, battery cell discharge voltage V_{dis}, power produced during eclipse $P_{eclipse}$, number of batteries used N_B and diodes voltage drop V_d (used for inter connection of battery cells) parameters will used as shown in the equation 5.7. Whereas, the capacity is measured in ampere-hour AH.[55]

$$Bat_{capacity} = \frac{P_{eclipse}t_{eclipse}}{N_BDoD(V_{dis}(N_c - 1) - V_d)}. \tag{5.7}$$

As most of the small satellites are launched in the LEO so the performance figure estimation is focused on for LEO here. The solar array mass M_{sa} and area A_{sa} is used for the estimation of performance of figure. While power produced at the end of life P_{EoL} is used for the calculations of performance figure as shown in the equation 5.8 [55] [56]

$$P_{SolarArray} = \frac{(A_{sa}^3 \times M_{sa}^2)}{P_{EoL}}. \tag{5.8}$$

In the power budget section, Aalto-1 CubeSat power requirement parameters are used for the budgeting. The power budget panel compute the total standby and peak power requirements along with the power generated and consumed during an orbital period and based on these computations, the operational time is estimated. The computation details have been explained in the section 3.4. The power budget tool also calculates the power requirements during the different phases of mission as configured in the tool. The figure 5.10 displays the Aalto-1 CubeSat power requirement estimations during the various phases of its operation.

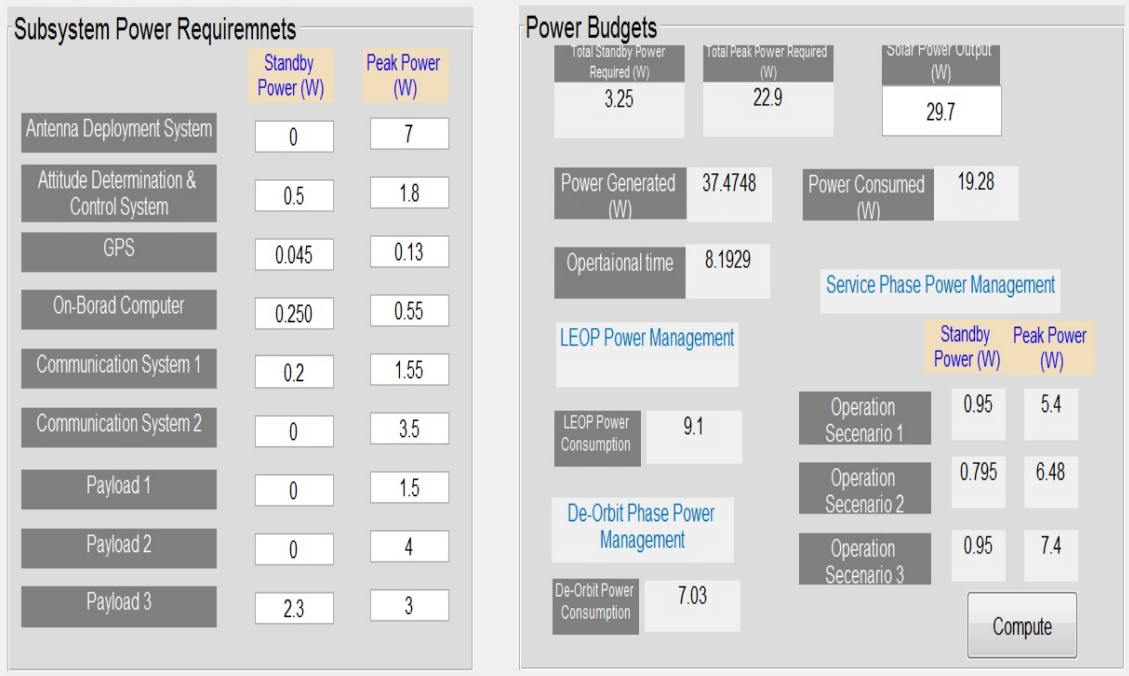

Figure 5.10: Power budget module of the satellite mission planning tool

Communication and Data Budget Calculations

The satellite planning tool has three sections for communication and data budgeting. In the ground station panel, GS latitude and longitude is provided while in configuration panel, various parameters are set to calculate the communication and data budgets. These parameters help to compute the effective antenna area, noise power, free-space loss, propagation delay, effective isotropic

radiated power (EIRP) and receive antenna power whereas, in the data budget section, on-board memory data download time is estimated considering the propagation delays and data rates. The data rates are estimated using the bandwidth information for QPSK coding schemes. The graphical user interface of communication and data budgets is shown in the figure 5.11.

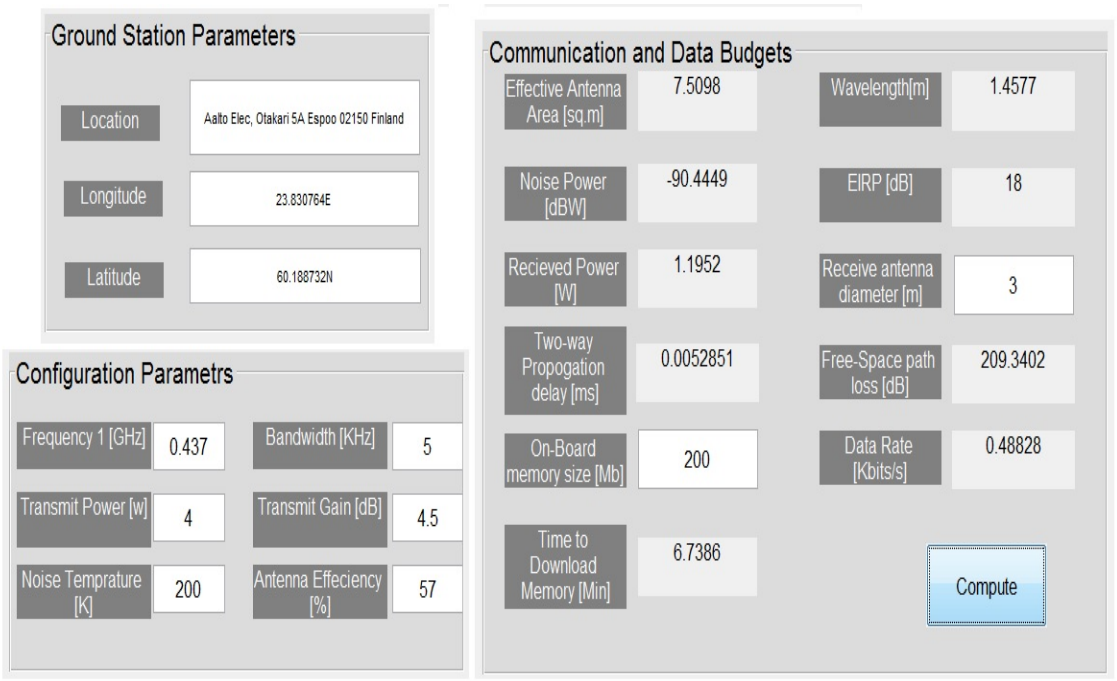

Figure 5.11: Communication and data budget module of the satellite mission planning tool

Chapter 6

Summary and Conclusions

6.1 Summary and Conclusions

Over the last decade, space technology has an exponential growth trend due to advances in electronics, sensor technology and cost effective solutions for construction and launch of spacecraft missions. The miniaturization of electronic components and sensors have emerged the new era for micro and nanosatellites research and development. Many space research organizations and universities all over the world have wide interest in the development of small satellite solutions for their future missions. Small satellite/CubeSat is the viable solution for universities who are focused on the in-house hardware and software development for their scientific experimentations. The main motivation behind this research thesis is to develop an optimized solution for the small satellite mission planning and scheduling during various mission phases focusing on the Aalto-1 CubeSat developed at Aalto University.

The thesis proposes a novel approach for the optimization of satellite mission scheduling and planning using genetic algorithm which can process substantial number of operational tasks. The algorithm provides an approach for the optimization of multi-objective mission scheduling. This technique can also be extended for the managing numerous missions at the same time with the optimized operational schedule. In this thesis, also a heuristic scheduling approach based on the constraint satisfaction problem (CSP) is presented to provide

an optimized solution for less complex operational tasks for satellites. Thesis research also focuses various satellite mission phases for the development and in-orbit operations promising the successful mission objectives. The study helps to reduce the risk of mission failures due to the lack of compliance of mission development standards and planning of operational tasks. Aalto-1 CubeSat mission has been the focus of study for the description of numerous mission design and in-orbit operations phases. Aalto-1 CubeSat power budgets, on-board data budgets and communication schemes have been elaborated in detail for the optimization of successful mission planning and scheduling.

The simulation results of genetic algorithm demonstrate the selection of task by evaluating the fitness function of each individual task based on their assigned weight factors and selecting the task depending on their score rank using tournament selection procedure. This method minimizes the constraints for the selection operator by improving the scores iteratively. This approach is very efficient to solve the complex scheduling tasks of muti-objective missions. GA optimization technique resolves the constraint scheduling problems within the short interval of time. The second technique for scheduling and planning optimization is heuristic approach based on the constraint satisfaction problem. In this technique, satellite scheduling task are modeled using two CSP solvers. The first CSP solver arrange the satellite subsystems operation with respect to their tasks. In this strategy, subsystem operations are taken as variable in their tasks domain which number of tasks and their preferences are taken as their constraint. The second CSP solver takes the input from the previous one and model the schedule task in the time domain using their time preference as constraint. The CSP based scheduling is viable solution for simple satellite operation without any complexities. When the tasks of multi-objective mission are more complex, the GA optimization techniques is preferred over the CSP because GA is more efficient to handle complex tasks within the short span of time.

In the scope of thesis work, a satellite mission planning tool is developed to provide aid for the scheduling tasks and budgeting of small satellite subsystems. The tool takes the TLE data form the NORAD and compute the keplerian elements and numerous orbital parameters required for the power budgets, data

budgets and communication link budgets. The power budget module estimates the satellite operational time base on the calculations of power generation, consumption and stored capacity. The power budget module also help to compute the power requirements during various in-orbit operational phases. The communication and data budget module computes the numerous RF and data link parameters which helps to estimate the data transfer to ground station during satellite pass over.

The Aalto-1 CubeSat mission is also simulated with the Systems Tool Kit (STK) software for the analysis of its orbital parameters and estimation of change in the angle between orbit plane and sun direction (β). The Euler angles has also been plotted to observe the change in the orientation of the satellite along with in-orbit eclipse time simulations. Gpredict software is used for simulations of orbit prediction data which computes the next pass of satellite using the TLE data. Gpredict software also provides the interface to operate the ground station antenna motor to establish the link with satellite. Sat Master Pro tool is used to estimate the link budgets to analyze the attenuation models and comparison of data rates using numerous modulation schemes.

The study verifies that small satellite missions are an excellent platform for both commercial as well as scientific research with its low cost development. A system engineering approach is discussed in detail for the small satellite mission design and in-orbit operational phases to address the issues related to many CubeSat mission failures due to lack of micro-management of resources and document control. The mission design also play an important role for the planning and scheduling of mission tasks. Two different techniques, i) Scheduling based on the Genetic Algorithm (GA) and, ii) Scheduling using Constraint-Based Approach, is discussed in detail. Both of these techniques can be used for the successful planning and scheduling of small satellite missions base on the complexity of the tasks. For Multi-objective missions, the task scheduling become complex for which GA is preferred due to its better optimization results. The GA is widely used in many other scheduling problem (e.g complex university time schedule, product production scheduling etc.). The optimized solution for the small satellite mission planning and scheduling of various mission phases has been implemented focusing on Aalto-1 CubeSat mission design.

A mission simulation software toolbox, utilizing the mentioned optimization techniques, has been developed in order to provide mission analysis tools for CubeSats. Consequently, Aalto-1 CubeSat power budgets, on-board data budgets and communication schemes for UHF and S-band have been analyzed to optimize the mission scheduling and planning for it's in orbit operations.

For the further improvements and future work, the genetic algorithm implantation can be extended for the multiple satellite missions to optimize their scheduling and operational tasks which helps to improve the ground station resources especially when Aalto-2 CubeSat mission will be launched and same Aalto-1 ground station can be efficiently utilized for the operations of both satellite, managing their operational task priority. The satellite mission planning tool can be extended by integrating Systems Tool Kit (STK) software using Matlab interface which will further enhance the capability of mission planning tool due to extensive simulation options available in STK. Furthermore, an additional panel can be added to integrate the GPredict software data for the prediction of next satellite passes.

Bibliography

[1] T. E. of ESA website. (2015). Space engineering and technology, [Online]. Available: http://www.esa.int/Our_Activities/Space_Engineering_Technology/CubeSats_offered_deep-space_ride_on_ESA_asteroid_probe (visited on 03/09/2015).

[2] S. L. et. al, "Cubesat design specification", California Polytechnic State University, CubeSat design Specification Rev. 13, 2014.

[3] S. Waydo, D. Henry, and M. Campbell, "Cubesat design for leo-based earth science missions", in *Aerospace Conference Proceedings, 2002. IEEE*, vol. 1, 2002, 1–435–1–445 vol.1. DOI: 10.1109/AERO.2002.1036863.

[4] V. Kolici, X. Herrero, F. Xhafa, and L. Barolli, "Local search and genetic algorithms for satellite scheduling problems", in *Broadband and Wireless Computing, Communication and Applications (BWCCA), 2013 Eighth International Conference on*, 2013, pp. 328–335. DOI: 10.1109/BWCCA.2013.58.

[5] S. Asundi and N. Fitz-Coy, "Cubesat mission design based on a systems engineering approach", in *Aerospace Conference, 2013 IEEE*, 2013, pp. 1–9. DOI: 10.1109/AERO.2013.6496900.

[6] E. C. for Space Standardization, "Space project management- project phasing and planning", ESA-ESTEC, The Netherlands, ECSS-M-30A, 1996.

[7] D. M. Klumpar, "Cubesat lessons learned: Two launch failures followed by one mission success (subtitle: What can go wrong will go wrong.)", Proceedings of the AIAA/USU Conference on Small Satellites, Session, 2012.

[8] A. Toorian, K. Diaz, and S. Lee, "The cubesat approach to space access", in *Aerospace Conference, 2008 IEEE*, 2008, pp. 1–14. DOI: 10.1109/AERO.2008.4526293.

[9] R. Torres, S. Lokas, D. Geudtner, and B. Rosich, "Sentinel-1a leop and commissioning", in *Geoscience and Remote Sensing Symposium (IGARSS), 2014 IEEE International*, 2014, pp. 1469–1472. DOI: 10.1109/IGARSS.2014.6946714.

[10] R. Haga and J. Saleh, "Epidemiology of satellite anomalies and failures: A subsystem-centric approach", in *Aerospace Conference, 2011 IEEE*, 2011, pp. 1–19. DOI: 10.1109/AERO.2011.5747656.

[11] S. mi Han, S. woo Beak, K. rae Cho, D.-W. Lee, and H. dong Kim, "Satellite mission scheduling using genetic algorithm", in *SICE Annual Conference, 2008*, 2008, pp. 1226–1230. DOI: 10.1109/SICE.2008.4654845.

[12] N. Bianchessi, J.-F. Cordeau, J. Desrosiers, G. Laporte, and V. Raymond, "A heuristic for the multi-satellite, multi-orbit and multi-user management of earth observation satellites", *European Journal of Operational Research*, vol. 177, no. 2, pp. 750 –762, 2007, ISSN: 0377-2217. DOI: http://dx.doi.org/10.1016/j.ejor.2005.12.026. [Online]. Available: http://www.sciencedirect.com/science/article/pii/S0377221706000051.

[13] J. C. Pemberton and I. Flavius Galiber, "A constraint-based approach to satellite scheduling", *Pacific-Sierra Research, Arlington, VA 22209*,

[14] R. Malhotra, N. Singh, and Y. Singh, "Genetic algorithms: Concepts, design for optimization of process controllers", *Computer and Information Science*, vol. 4, no. 2, pp. 39–54, 2011.

[15] T. E. of Matlab MathWorks. (2015). Genetic algorithm, [Online]. Available: http://se.mathworks.com/discovery/genetic-algorithm.html (visited on 03/09/2015).

[16] R. Barták, "Constraint-based planning and scheduling", 22nd International Conference on Automated Planning and Scheduling, Atibaia, Sao Paulo Brazil, 2012.

[17] A. Mackworth and E. Freuder, "The comlexity of some polynomial network consistency algorithms for constraint satisfaction problems", *Artificial Intelligence, Elsevier Science Publishers B.V. (North Holland)*, vol. 25, 1985.

[18] A. Kestilä, T. Tikka, P. Peitso, J. Rantanen, A. Nasil, K. Nordling, H. Saari, R. Vainio, P. Janhunen, J. Praks, and M. Hallikainen, "Aalto-1 nanosatellite technical description and mission objectives", *Geoscientific Instrumentation, Methods and Data Systems*, vol. 2, no. 1, pp. 121–130, 2013. DOI: 10.5194/gi-2-121-2013. [Online]. Available: http://www.geosci-instrum-method-data-syst.net/2/121/2013/.

[19] A. Näsilä, A. Hakkarainen, J. Praks, A. Kestilä, K. Nordling, R. Modrzewski, H. Saari, J. Antila, R. Mannila, P. Janhunen, R. Vainio, and M. Hallikainen, *Aalto-1: A hyperspectral earth observing nanosatellite*, 2011. DOI: 10.1117/12.898125. [Online]. Available: http://dx.doi.org/10.1117/12.898125.

[20] T. T. Kimmo Karvinen and J. Praks, "Using hobby prototyping boards and commercial-off-the-shelf (cots) components for developing low-cost, fast-delivery satellite subsystems", *Journal of Small Satellites (JoSS)*, vol. 4, no. 1, pp. 301–314, 2015.

[21] H. Saari, K. Viherkanto, R. Mannila, C. Holmlund, J. Antila, and I. Näkki, "Aalto-1 science mission of aalto-1 imaging spectrometer", VTT Technical Research Centre of Finland, Aalto-1 design document A1-SPE-RS-01-v2, 2012.

[22] J. Praks, A. Kestila, M. Hallikainen, H. Saari, J. Antila, P. Janhunen, and R. Vainio, "Aalto-1 - an experimental nanosatellite for hyperspectral remote sensing", in *Geoscience and Remote Sensing Symposium (IGARSS), 2011 IEEE International*, 2011, pp. 4367–4370. DOI: 10.1109/IGARSS.2011.6050199.

[23] R. Vainio, "Aalto-1 science mission plan for radmon", University of Helsinki and Turku, Aalto-1 design document Doc. No. A1-RAD-PL-03-v1-DRAFT, 2011.

[24] P. Janhunen, *Electric sail propulsion modeling and mission analysis*, 2007.

[25] J. P. Osama Khurshid Tuomas Tikka and M. Hallikainen, "Accommodating the plasma brake experiment on-board the aalto-1 satellite", in *Proceedings of the Estonian Academy of Sciences*, ser. 63, vol. 2S, Estonia, 2014, 258–266.

[26] J. Envall, "Aalto-1 science mission of electrostatic plasma brake", Finnish Meteorological Institute, Aalto-1 payload design document Doc. No. A1-EPB-PL-03-v3, 2013.

[27] B. S. Technologies. (2015). Iadcs-100, intelligent attitude control for cubesats., [Online]. Available: `www.berlin-space-tech.com/fileadmin/media/BST_iACDS-100_Flyer.pdf` (visited on 07/02/2015).

[28] F. MP. (2008). Gps receiver hardware and application development products, [Online]. Available: `www.farnell.com/datasheets/301082.pdf` (visited on 07/02/2015).

[29] J. Finnholm, J. Hemmo, T. Nikkanen, and M. Komu, "Aalto-1 design of the electrical power system", Aalto University Finland, Aalto-1 design document A1-EPS-DD-02-v2, 2013.

[30] E. Sorva and J. Finnholm, "Aalto-1 solar panel flight model manufacturing process", Aalto University Finland, Aalto-1 design document A1-EPS-MA-02-v1, 2015.

[31] J. Finnholm and E. Sorva, "Aalto-1 solar panel test readiness review", Aalto University Finland, Aalto-1 Test document A1-TRR-Solar-Panels, 2015.

[32] A. Strain, V. McLaren, and P. Marinov, "User manual: Cubesat 3u electronic power system cs-3ueps2-nb", Clyde Space, Document No.: USM-0007, 2011.

[33] L. ClydeSpace. (2015). Cubesat standalone battery 30whr, [Online]. Available: `http://www.clyde-space.com/cubesat_shop/batteries/279_cubesat-standalone-battery` (visited on 06/16/2015).

[34] S. Ian, E. Razzaghi, O. Khurshid, and A. Kestilä, "Design of the on board computer hardware", Aalto University Finland, Doc. No. A1-OBH-DD-01-v4, 2012.

[35] P. Semiconductors. (2006). I2C Bus i2c bus typical setup, [Online]. Available: `http://www.i2c-bus.org/i2c-primer/typical-i2c-bus-setup/` (visited on 07/25/2015).

[36] P. Niemelä, N. Silva, H. Leppinen, and A. Kestilä, "Aalto-1 design of the on-board computer software", Aalto University Finland, Doc. No. A1-OBS-DD-01-v4, 2015.

[37] H. Sanmark, N. Silva, P. Niemelä, O. Khurshid, S. Lan, A. Yanes, A. Ilmanen, and H. Leppinen, "Aalto-1 obc payload communication protocol definitions and details", Aalto University Finland, Doc. No. A1-OBH-DS-03-v4, 2013.

[38] H. Sanmark, N. Silva, and P. Niemelä, "High-level design of the aalto-1 on-board computer software", Aalto University Finland, A1-OBS-DD-03-v1, 2014.

[39] Ficora. (2015). Frequency allocations, [Online]. Available: `https://www.viestintavirasto.fi/en/spectrum/radiospectrumuse/frequencyallocationtable.html` (visited on 07/23/2015).

[40] J. Jussila, "S-band transmitter for aalto-1 nanosatellite", diploma thesis, School of Electrical Engineering, Aalto University Finland, 2013.

[41] A. Näsilä, "Preliminary design of the radio communication system part 2: Vhf/uhf radio", Aalto University Finland, Doc. No. A1-COM-DD-02-v2, 2011.

[42] M. Lankinen, "Preliminary design of the radio communication system part 4: Vhf/uhf antennas", Aalto University Finland, Doc. No. A1-COM-IF-02-v3, 2011.

[43] R. Modrzewski, "Preliminary design of the radio communication system part 3: S-band antenna", Aalto University Finland, Doc. No. A1-COM-DD-03-v3, 2011.

[44] A. Näsilä, "Preliminary design of the radio communication system part 1: S-band radio", Aalto University Finland, Doc. No. A1-COM-IF-01-v3, 2011.

[45] G. S. Administration, *F. s. 1037c, earth station.*

[46] I. T. U. (ITU). (2015). Itu radio regulations – article 1, definitions of radio services, [Online]. Available: `http://www.ictregulationtoolkit.org/en/toolkit/notes/PracticeNote/2824` (visited on 07/12/2015).

[47] A. Näsilä and P. Niemelä, "Aalto-1 design of ground station", Aalto University Finland, Doc. No. A1-GND-DD-01-v3, 2015.

[48] Arrowe. (2015). Satmaster pro satellite link budget software, [Online]. Available: `http://www.eletrica.ufpr.br/evelio/TE111/Eb_N0.pdf` (visited on 07/25/2015).

[49] J. Pearce. (2000). Eb/n0 explained, [Online]. Available: http://www.eletrica.ufpr.br/evelio/TE111/Eb_N0.pdf (visited on 07/18/2015).

[50] A. Csete. (2009). Gpredict satellite tracking and orbit prediction, [Online]. Available: http://gpredict.oz9aec.net/index.php (visited on 07/15/2015).

[51] J. J. Blanco and L. Khatib, "Course scheduling as a constraint satisfaction problem", in *In Proc. PACT98*, 1998.

[52] C. Clark and R. Logan. (2011). Power budgets for mission success, [Online]. Available: www.clyde-space.com/documents/2276 (visited on 06/15/2015).

[53] S. Arnold, R. Nuzzaci, and A. Gordon-Ross, "Energy budgeting for cubesats with an integrated fpga", in *Aerospace Conference, 2012 IEEE*, 2012, pp. 1–14. DOI: 10.1109/AERO.2012.6187240.

[54] W. J. R. Larson Wiley J., *Space mission analysis and design*, ed. CA: Microcosm, 1999.

[55] S. Asif, Y. Li, and J. Zhang, "Intelligent search and multi-criteria optimisation of spacecraft power subsystems", Proceedings of the 12th Chinese Automation and Computing Society Conference in the UK, Loughborough, England, 16 September 2006, 2006.

[56] M. Reddy, "Space solar cells—tradeoff analysis", *Solar Energy Materials and Solar Cells*, vol. 77, no. 2, pp. 175 –208, 2003, ISSN: 0927-0248. DOI: http://dx.doi.org/10.1016/S0927-0248(02)00320-3. [Online]. Available: http://www.sciencedirect.com/science/article/pii/S0927024802003203.